AGU PUBLICATIONS

JGR

Journal of Geophysical Research: Biogeosciences

RESEARCH ARTICLE
10.1002/2015JG003002

Key Points:
- Simulations evaluate meteorologic variability on water/carbon fluxes and stores
- Cross-scale information transfer is ecosystem/resource-limitation dependent
- Fast meteorological drivers affect long-term fluxes when stores are affected

Supporting Information:
- Supporting Information S1
- Data Set S1

Correspondence to:
A. Paschalis,
athanasios.paschalis@duke.edu

Citation:
Paschalis, A., S. Fatichi, G. G. Katul, and V. Y. Ivanov (2015), Cross-scale impact of climate temporal variability on ecosystem water and carbon fluxes, *J. Geophys. Res. Biogeosci.*, *120*, 1716–1740, doi:10.1002/2015JG003002.

Received 26 MAR 2015
Accepted 4 AUG 2015
Accepted article online 7 AUG 2015
Published online 5 SEP 2015

Cross-scale impact of climate temporal variability on ecosystem water and carbon fluxes

Athanasios Paschalis[1,2], Simone Fatichi[2], Gabriel G. Katul[1,3], and Valeriy Y. Ivanov[4]

[1]Nicholas School of the Environment, Duke University, Durham, North Carolina, USA, [2]Institute of Environmental Engineering, ETH Zurich, Zurich, Switzerland, [3]Department of Civil and Environmental Engineering, Duke University, Durham, North Carolina, USA, [4]Department of Civil and Environmental Engineering, University of Michigan, Ann Arbor, Michigan, USA

Abstract While the importance of ecosystem functioning is undisputed in the context of climate change and Earth system modeling, the role of short-scale temporal variability of hydrometeorological forcing (~1 h) on the related ecosystem processes remains to be fully understood. Various impacts of meteorological forcing variability on water and carbon fluxes across a range of scales are explored here using numerical simulations. Synthetic meteorological drivers that highlight dynamic features of the short temporal scale in series of precipitation, temperature, and radiation are constructed. These drivers force a mechanistic ecohydrological model that propagates information content into the dynamics of water and carbon fluxes for an ensemble of representative ecosystems. The focus of the analysis is on a cross-scale effect of the short-scale forcing variability on the modeled evapotranspiration and ecosystem carbon assimilation. Interannual variability of water and carbon fluxes is emphasized in the analysis. The main study inferences are summarized as follows: (a) short-scale variability of meteorological input does affect water and carbon fluxes across a wide range of time scales, spanning from the hourly to the annual and longer scales; (b) different ecosystems respond to the various characteristics of the short-scale variability of the climate forcing in various ways, depending on dominant factors limiting system productivity; (c) whenever short-scale variability of meteorological forcing influences primarily fast processes such as photosynthesis, its impact on the slow-scale variability of water and carbon fluxes is small; and (d) whenever short-scale variability of the meteorological forcing impacts slow processes such as movement and storage of water in the soil, the effects of the variability can propagate to annual and longer time scales.

1. Introduction

Climate varies across a wide range of temporal and spatial scales [*McManus*, 1999], and this variability affects and is affected by vegetation. In particular, the carbon cycle is sensitive to climate variability through multiple processes operating on different time scales such as vegetation growth, mortality, and competition [*Wilson and Baldocchi*, 2000; *Bonan*, 2008; *Sitch et al.*, 2008; *Arora et al.*, 2013; *Friedlingstein et al.*, 2014]. Considering the rapid change in climate and its variability as projected by the last generation climate models [*Intergovernmental Panel on Climate Change*, 2013], it is becoming necessary to quantify the associated responses of ecosystems in terms of water and carbon fluxes and their feedback to the climate [*Medvigy et al.*, 2010; *Reichstein et al.*, 2013]. The importance of these responses is potentially large, given the potential economic and societal effects resulting from loss of wood yield or food production, and accelerated desertification of semiarid areas, to name a few.

The statistical features of climatic forcing such as air temperature and precipitation evolve in terms of magnitude and variability [*Karl et al.*, 1995; *Boer*, 2009; *Medvigy and Beaulieu*, 2012; *Sun et al.*, 2012; *Cattiaux et al.*, 2015]. Changes concerning climate variability include alternation of precipitation and temperature extremes [*Allan and Soden*, 2008; *O'Gorman and Schneider*, 2009; *Kharin et al.*, 2013], changes in precipitation frequency [*Sun et al.*, 2007] and amounts, changes in the diurnal patterns of temperature and humidity [*Vinnikov*, 2002; *Cattiaux et al.*, 2015; *Fatichi et al.*, 2015], and changes in the variability of the incoming solar radiation [*Medvigy and Beaulieu*, 2012], among others. In particular, variability at the short temporal scales (e.g., intraannual to subdaily) has been found to have a major significance for ecosystems [*Medvigy et al.*, 2010; *Fatichi and Ivanov*, 2014; *Vico et al.*, 2014]. Variability at such scales is also essential for the hydrological cycle, which in turn influences vegetation in different ways across biomes.

The variability of the meteorological forcing can affect ecosystem functions in various ways. For example, precipitation structure determines the root zone soil water availability, which in turn affects plant productivity and thus carbon and water fluxes through photosynthesis and transpiration [*Fay et al*., 2000; *Huxman et al*., 2004b]. Temperature variability at small scales (e.g., hours to days), and the temperature correlation structure defining cold or heat wave persistence, can affect vegetation productivity and water fluxes (e.g., evapotranspiration) through its impact on the energy balance of the ecosystem, as well as biochemical processes related to carbon fluxes (e.g., photosynthesis and respiration) [*Asseng et al*., 2011]. Changes in temperature diurnal patterns have been also found to affect vegetation functioning and soil biogeochemistry [*Collatz et al*., 2000; *Peng et al*., 2013; *Xia et al*., 2014]. Radiation variability at the small temporal scales (e.g., hours to days) can also affect the energy balance of the ecosystems, because of the nonlinearity embedded in radiation dependent processes.

The responses of ecosystems to environmental drivers are generally difficult to quantify due to the large number of nonlinear feedback among biological, ecological, and hydrological processes occurring at multiple scales [*Eagleson*, 1978; *Laio et al*., 2001; *Rodriguez-Iturbe et al*., 2001; *Katul et al*., 2007b; *Thornton et al*., 2014]. Early studies attempted to relate the amount of water and carbon fluxes to mean annual environmental drivers with the goal of extrapolating them to future climates [*Fang et al*., 2001; *Knapp and Smith*, 2001; *Huxman et al*., 2004a]. Arguably, the most common relation in hydrology is the Budyko's curve [*Donohue et al*., 2007; *Li et al*., 2013] that relates long-term evaporation to dryness indices.

It is widely recognized that Budyko's curve or similar empirical relations have predictive skill at the global scale and are able to unfold connections between resource limitations (energy versus water) when discerning some ecosystem responses (e.g., water loss). However, their predictive skill degrades at local scales due to the influence of heterogeneities in forcing and boundary conditions, which affect water and carbon fluxes and storage at smaller spatial and temporal scales [*Knapp and Smith*, 2001; *Stoy et al*., 2006; *Brooks et al*., 2011; *Fatichi and Ivanov*, 2014; *Pappas et al*., 2015]. The recognition that short-scale climate variability impacts ecosystem functioning [*Huxman et al*., 2004b; *Jentsch et al*., 2007; *Medvigy et al*., 2010] has led to significant advances in eco-hydrology and motivates this study.

To assess the relevance of short-scale variability of environmental drivers on carbon-water fluxes and storage, several experimental studies have been conducted. Results from these experiments highlight the significance of short-scale temporal variability and statistical structure of precipitation on vegetation dynamics [*Swemmer et al*., 2007; *Heisler-White et al*., 2008; *Fay et al*., 2011] and the role of temperature distribution and structure (e.g., diurnal variations) [*Wan et al*., 2002; *De Boeck et al*., 2010; *Wu et al*., 2011; *Peng et al*., 2013; *Xia et al*., 2014]. Even though experiments provide necessary information about vegetation response to climatic fluctuations, technical and resource limitations typically constrain generality of such experiments. In particular, the complexity of the soil-vegetation-atmosphere system precludes the experimental manipulation of many of the existing feedback between biological and hydrological processes.

In the last decade, simultaneous advances in understanding ecosystem functioning and the increases in computational capabilities have led to the development of numerical models that resolve the essential hydrological and ecological processes at the relevant scales [*Sitch et al*., 2003; *Krinner et al*., 2005; *Ivanov et al*., 2008; *Fatichi et al*., 2012b]. These models offer practical tools to construct and test hypotheses about the role of short-scale variability in hydrological, ecological, and climate studies [*Sitch et al*., 2008; *Gonzalez et al*., 2010; *Medvigy et al*., 2010]. A major advantage of using such models is that known feedback between soil, vegetation, and the atmosphere can be quantified, and thus, a generalized assessment concerning the influence of the variability of the environmental drivers on water and carbon fluxes can be outlined.

Using one of such mechanistic models, the overarching question we address here is how short-scale and interannual variability of meteorological forcing affects water and carbon fluxes of various ecosystems spanning a range from boreal forests to semiarid shrublands. The focus is on precipitation, temperature, and radiation because the responses of ecosystems to these environmental variables are reasonably well understood. Other variables that evolve slowly in time such as the atmospheric CO_2 are not considered. Also, other features of the high-frequency variability, such as spring frost damage, known to be impacted by rapid excursions in air temperature variability, are not explicitly considered [*Rigby and Porporato*, 2008].

The elements of hydrometeorologic variability investigated here are (i) the interannual variability of the climate forcing; (ii) the autocorrelation and crosscorrelation of hourly precipitation, temperature, and

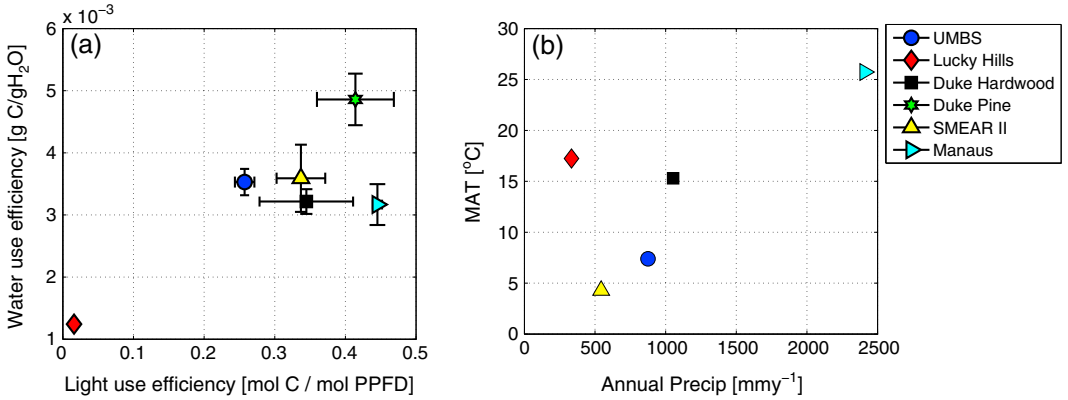

Figure 1. (a) Water use efficiency and light use efficiency defined as the ratios of annual GPP to annual transpiration and annual incoming photosynthetic active radiation, respectively, and (b) mean annual precipitation and mean annual air temperature for the analyzed stations. Error bars correspond to the annual standard deviations.

radiation; (iii) the precipitation structure, and its intermittency patterns (i.e., organization in storm events); and (iv) the probability distribution of precipitation, temperature, and radiation, with an emphasis on their extremes. The analysis is based on a comprehensive numerical experimentation with the state-of-the-science Tethys-Chloris (T&C) ecohydrological model [*Fatichi*, 2010; *Fatichi et al*., 2012b], a tool that integrates essential hydrological and plant physiological processes. The effects of temporal variability of climatic forcing on evapotranspiration (ET), and its partition into subcomponents, and plant productivity are the main focus. Physical interpretations of the mechanisms that affect ET and plant productivity for the analyzed ecosystems across temporal scales are provided. As a practical outcome for planning future field (and numerical) experiments, we seek generalizations that can be used as guidelines for assessing ecosystem responses to a changing climate [*Smith et al*., 2014; *Kayler et al*., 2015].

2. Case Studies and Data

Data from six biomes located in five different sites are used. The sites investigated are (i) a deciduous forest at the University of Michigan Biological Station (UMBS) in Michigan, USA; (ii) a boreal pine forest in the Hyytiälä field station (SMEAR II) in southern Finland; (iii) a semiarid shrubland in Lucky Hills, Arizona, USA; (iv) a tropical rainforest near Manaus, Brazil; and (v) an evergreen pine stand and a deciduous hardwood forest near Durham (Duke Forest), North Carolina, USA. In Figure 1, a brief summary of the sites and their climate is provided (Figure 1b) as well as the simulated annual water use and light use efficiency (Figure 1a). Data from these sites have been extensively analyzed before [*Scott et al*., 2000; *Oren et al*., 2001; *Yuan et al*., 2007; *Ivanov et al*., 2010; *Restrepo-Coupe et al*., 2013], and only a brief description is provided here.

Lucky Hills (110.30°W, 31.44°N; elevation 1372 m above sea level (asl)) is located in the Walnut Gulch experimental catchment in Arizona [*Keefer et al*., 2008; *Renard et al*., 2008; *Paschalis et al*., 2014b]. Vegetation in this site is sparse and consists of various types of shrubs (deciduous whitethorn acacia and evergreen tarbush, and creosotebush). The soil type is sandy-loam with a relatively low water holding capacity and high permeability [*Ritchie et al*., 2005]. The assumed soil depth is 2 m, and root-zone depth is 0.9 m. Vegetation productivity in Lucky Hills is limited by water availability due to low precipitation and its uneven distribution during the year controlled by the North American Monsoon and also due to a high evaporative demand. Meteorological data for the time period 1996–2009, collected by United States Department of Agriculture-Agricultural Research Service, Southwest Watershed Research Center, are used.

The deciduous forest in UMBS (84.71°W, 45.55°N; elevation 234 m asl.) consists primarily of aspen trees, and a smaller fraction of northern red oak, paper birch, American beech, sugar maple, red maple, and white pine [*Curtis et al*., 2005; *Gough et al*., 2008, 2013; *Fatichi and Ivanov*, 2014]. The soil in the forest is sandy (98% sand), with a low percentage of organic matter and small water holding capacity [*Pregitzer et al*., 1993]. The assumed soil depth is 3 m, and root-zone depth is assumed to be 0.8 m [*He et al*., 2013]. Plant productivity in UMBS is mostly limited by low temperatures. For this site, 12 years of available data (1999–2010) were used. Meteorological and eddy covariance data were collected at the 33 m tall tower, part of AmeriFlux.

The tropical rainforest site (60.21°W. 2.61°S; elevation 67 m asl.) is located in the Cuieiras reserve near Manaus in Northern Brazil and is part of the Large-Scale Biosphere Atmosphere Experiment in Amazonia (LBA). Vegetation consists primarily of broadleaf evergreen trees [*Araújo et al*., 2002]. The soil consists of a nutrient poor deep clayey soil. The root system of the trees in the Amazon rain forest is known to be extensive and have access to the deep water storage even during the dry season [*Nepstad et al*., 1994; *Markewitz et al*., 2010; *Ivanov et al*., 2012], potentially enhanced by processes such as hydraulic lift [*Oliveira et al*., 2005; *Yan and Dickinson*, 2014]. Meteorological and flux data are collected at a 50 m tall tower (FLUXNET site: Manaus - ZF2 K34) operating since 1999. Vegetation productivity at this site is assumed to be light limited, even though nutrients may play a very important role on this ecosystem [*Körner*, 2009]. In particular, enhanced carbon gain typically occurs during the dry season when light availability is higher and photosynthesis is likely to be more efficient [*Saleska et al*., 2003, 2007; *Hutyra et al*., 2007; *Myneni et al*., 2007; *Kim et al*., 2012]. However, results that indicate that the rainforest in Manaus may not be particularly limited by radiation, as has also been reported by *Restrepo-Coupe et al*. [2013]. In this study, the soil depth was assumed to extend to 14 m and the root depth to 10 m. Meteorological data for the time period 1999–2005 are used.

The SMEAR II site (24.17°E, 61.51°N; elevation 181 m asl.) is located in a Scots pine plantation in southern Finland established in 1962 [*Pumpanen et al*., 2003; *Kolari et al*., 2004]. The soil is a low fertility silty sand confined by an impermeable bedrock [*Pumpanen et al*., 2003; *Suni et al*., 2003]. The soil depth is assumed to extend to 3 m and the root zone to 0.8 m. Hydrometeorological and flux data for this site were measured at a 73 m tower from 1996 to 2013, operated by the University of Helsinki. The main limitations to photosynthesis are light availability due to the high latitude, low temperature and, occasionally, by low water availability, due to the relatively small precipitation.

Finally, two adjacent sites located within the Duke Forest (79.09°W, 35.98°N, 168 m asl; pine forest and hardwood forest) are also explored as these sites represent similar climate and soil type but different vegetation covers. The first is a loblolly pine plantation established in 1983 from 3 year old seedlings [*Pritchard et al*., 2008]. The understory of this loblolly pine forest consists of several deciduous species (red maple, sweetgum, tulip poplar, and redbud) that have established since then. The other site is a second-growth 120 year old southern oak-hickory hardwood forest that consists of several unevenly aged deciduous species such as tulip poplar, hickory, various types of oaks (white, chestnut, and willow), and sweetgum [*Palmroth et al*., 2005; *Stoy et al*., 2007]. The soil type of all sites is a shallow, nutrient poor silt loam with an impermeable clay pan at ~30 cm depth [*Oishi et al*., 2010] that formed due to prior land use history. Meteorological data were obtained at adjacent flux towers installed at each site as part of the global micrometeorological measurement network FLUXNET [*Baldocchi et al*., 2001] over the period 1998–2008 and operated by Duke University. Vegetation productivity at the Duke Forest during the period when leaves are present is not clearly limited by any environmental factor due to above freezing temperatures for most of the year, and high light and water availability. Air temperature and radiation (day-length) are controlling factors of the phenological status of the hardwood forest. Phenology is explicitly resolved in the used model, but it is only marginally impacted by high-frequency variations, due to the assumed parameterizations.

For all the sites used in this study, with the exception of Manaus, gaps in the meteorological data did not exceed 5%. Missing values for all meteorological variables except precipitation were filled with linear interpolation from their neighboring hourly observations, when the gaps were isolated, or given their mean climatological value, preserving the seasonality, and the diurnal cycle, in the cases where continuous gaps of data were present. For precipitation, missing values were filled with zeros. Given the very small number of gaps, the influence of the gap filling process is considered negligible. For Manaus, the data gaps were larger, and the procedure of gap filling is identical to the LBA Data Model Intercomparison Project [*de Gonçalves et al*., 2013].

3. Methods

The sensitivity of ecosystem responses in terms of water and carbon fluxes to the short temporal scales (~1 h) and the interannual variability of climate is assessed with a particular emphasis on precipitation, temperature, and incoming shortwave radiation. The sensitivity is studied using numerical simulations carried out with a state-of-the-science mechanistic ecohydrological model. The general principle guiding the simulations is that synthetic climate time series with prescribed statistical properties are used to drive the model, which yields responses that mimic ecosystem responses to the changed forcing conditions. The model has been

previously calibrated and evaluated for several sites considered here, and a summary of the evaluation for all of the sites is included in the supporting information. The total rainfall amount, total radiation, and long-term temperature are preserved across runs for each site. The corresponding statistical distributions and correlation structure in time are the variables that were synthetically varied here.

3.1. Ecohydrological Model and Vegetation Representation

The mechanistic ecohydrological model Tethys-Chloris (T&C) [*Fatichi*, 2010; *Fatichi et al*., 2012a, 2012b] is employed because this model has been shown to reproduce satisfactorily the fluxes of energy, carbon, and water across a wide range of temporal scales in many sites worldwide [*Fatichi and Leuzinger*, 2013; *Fatichi and Ivanov*, 2014; *Fatichi et al*., 2014a; *Pappas et al*., 2015]. Here only a brief description of the model is provided for reference; the details of its mathematical formulation can be found elsewhere [*Fatichi*, 2010; *Fatichi et al*., 2012a]. T&C simulates the essential hydrological and ecological processes regulating the water and carbon cycles. In particular, the model resolves the water and energy budgets at the soil and land surface and also accounts for vegetation dynamics. Meteorological variables required by the model are hourly time series of precipitation, temperature, incoming shortwave radiation, air temperature, wind speed, cloudiness, relative humidity, and atmospheric pressure above the canopy.

The modeled hydrological processes include saturated and unsaturated soil water flow and overland flow, interception, throughfall, snow hydrology, and a full solution of energy fluxes at the land surface. The result of this solution is a detailed quantification of the water fluxes between the soil/canopy and the atmosphere. The modeled pathways include water flow in the soil computed from Richards equation modified to include a distributed sink term representing root uptake and soil evaporation but without accounting for hydraulic redistribution. Soil depth and root zone depth are model parameters assigned to best represent local pedology and vegetation characteristics. Overland flow is estimated by solving the kinematic wave approximation of the Saint Venant equation. Interception and throughfall are modeled as a function of precipitation intensity and leaf area index. The solution of the energy balance, which also affects snow accumulation and melt, is performed using a resistance scheme analogue [*Sellers et al*., 1996]. In the present version of T&C, five resistances (atmospheric, under-canopy, soil, stomatal, and leaf boundary) are used and only one radiative temperature is estimated per time step. Even though T&C was developed to operate at the catchment scale and account for the influence of complex topography on radiation distribution (e.g., shading) and lateral water flow, flat terrain is assumed as a close approximation for all flux tower sites considered here.

T&C can use the concept of plant functional types (PFTs) or species specific parameters and conceptualizes vegetation structure as a series of interconnected carbon pools, a methodology commonly used in dynamic global vegetation models [*Haxeltine and Prentice*, 1996; *Sitch et al*., 2003; *Krinner et al*., 2005; *Oleson et al*., 2013]. Biomass in various plant carbon pools (leaves, fine roots, living sapwood, nonstructural carbohydrates, etc.) is estimated in a prognostic manner based on a system of differential equations that regulate carbon inputs (photosynthesis), losses (respiration and tissue turnover), and translocation among them, which follow a set of allometric, resource availability, and phenology status and rules. Photosynthesis is modeled using the widely accepted biochemical model at the leaf scale presented by *Farquhar et al*. [1980], including some modifications [*Collatz et al*., 1991; *Dai et al*., 2004; *Kattge and Knorr*, 2007; *Bonan et al*., 2011]. Photosynthesis can be reduced during drought stress periods, which are defined as periods when the soil water potential drops below a plant specific threshold. This photosynthetic reduction is based on a reduction factor that varies linearly with the soil moisture available to the roots, which is a function of root and soil moisture vertical distributions. Intercepted water inhibits transpiration [*Deardorff*, 1978] but does not inhibit CO_2 uptake except for the case when the canopy is at least 50% covered with snow. Carbon maintenance and growth respiration fluxes are modeled as a function of temperature, living biomass for every carbon pool and their carbon to nitrogen ratio [*Krinner et al*., 2005; *Fatichi*, 2010]. Biomass allocation in leaves is translated into a dynamic behavior of the leaf area index (LAI) based on the specific leaf area index, while other plant characteristics, such as plant height and root distribution, are maintained "static." Vegetation dynamics are affected by environmental forcing and are coupled with the main hydrological processes. Soil biogeochemistry and nutrient cycles are not explicitly simulated; thus, the model assumes vegetation to be in equilibrium with its nutritional environment. A detailed description of the model can be found elsewhere [*Fatichi*, 2010; *Fatichi et al*., 2012a, 2012b].

Table 1. Summary of the Meteorological Input Scenarios

	Combined cases	
1	*Control scenario*:	Observed data
2	*Periodic input*:	All inputs preserve only the diurnal and seasonal variability of precipitation, temperature, and radiation.
3	*Randomized input*:	Precipitation, temperature, and incoming radiation are simultaneously randomized by sampling without replacement, while preserving the seasonal and diurnal cycle and their conditional distributions.
	Precipitation	
4	*Randomized precipitation*:	Precipitation is randomized with sampling without replacement, while preserving the interannual, seasonal, and diurnal cycles.
5	*No IAV of precipitation*:	Interannual variability of precipitation is removed from the observed time series.
6	*More peaky precipitation*:	Precipitation peaks are enhanced by employing a probability transform, while preserving the interannual variability of precipitation.
7	*Less peaky precipitation*:	Peaks of precipitation are reduced by applying a moving average filter of 12 h. The interannual variability, and approximately the distribution of depth per event, is preserved.
	Temperature	
8	*Randomized temperature*:	Temperature series are randomized with sampling without replacement, while preserving the interannual, seasonal, and diurnal cycles.
9	*No IAV of temperature*:	Interannual variability of temperature is removed from the observed time series.
10	*Less extreme temperature*:	A moving average filter of 12 h is applied to the temperature time series.
	Radiation	
11	*Randomized radiation*:	Radiation series are randomized with sampling without replacement, while preserving the interannual, seasonal, and diurnal cycles.
12	*No IAV of radiation*:	Interannual variability of radiation is removed from the observed time series.

Initial conditions (carbon pools and soil water) for all the model runs were selected such that they represent realistic mature ecosystems in balance with their observed meteorological forcing; i.e., they are in a quasi-steady-state equilibrium.

3.2. Climate Forcing

The main focus is on the effect of interannual and short-scale (~1 h) climate variability on water and carbon fluxes. To conduct such an assessment, a series of synthetic climate inputs that manipulate the statistical structure of precipitation, temperature, and radiation are used to drive T&C. In particular, 12 different input cases are evaluated (Table 1), where the spectral and probabilistic structure of the climatic variables and their coherence with other climatic drivers are modified. The first case corresponds to the observed climate input and represents the benchmark, referred to as the control scenario throughout the manuscript. In the next 2 of the 12 cases, we simultaneously alter all climate forcing types, while in the remaining 9 cases, the effect of each of the variables of interest is separately modified, preserving the consistency of the other climatic variables with the measurements. Seasonality is a deterministic mode of temporal variability that influences ecosystem functioning. In the present study, we eliminated this degree of freedom from simulations and in all of the scenarios seasonal patterns of all climate variables are guaranteed to be identical to the observed series. The simulation length for all the cases is set to that of the observed series, and for the cases where random sampling was used, five ensembles were simulated to mimic stochastic variability.

3.2.1. Combined Cases

For the two cases where all climatic variables are simultaneously perturbed, the focus is on the combined effect of small-scale variability and the correlation structure (i.e., autocorrelation and cross correlations among all climatic variables) of the input.

In the second case (Table 1), the interannual variability along with the short-scale variability of precipitation, temperature, and radiation are suppressed. This is achieved by forcing the model with periodic input of the three variables of interest in which only the two dominant modes of variability, the seasonal and the diurnal, are retained so that

$$C_h^m(t) = \frac{1}{n}\sum_{i=1}^{n} Co_h^m(i) \tag{1}$$

where $C_h^m(t)$ is the climate variable of the $t-$th time step corresponding to the $m-$th month and $h-$th hour, and $Co_h^m(i)$ is the observed variable at the $i-$th time step corresponding to hour h and month m, and n is the total number of time steps for a specific month and hour. This input scenario serves as an indication as to whether carbon dynamics and water fluxes can be predicted from the mean values of the climatic forcing. Moreover, it can illustrate the importance of the overall climate variability for water and carbon fluxes.

In the third case, the correlation structure of the model input is altered by randomizing the three variables of interest (i.e., precipitation, temperature, and radiation) in time, specifically, using sampling without replacement. Sampling without replacement is used since we seek to preserve exactly the observed meteorological values without repetitions that would arise from sampling with replacement. For this case, two subcases are taken into account. In the first subcase, we randomize simultaneously in time all the three variables of interest. If $I = \{i_1, i_2, \ldots, i_n\}$ are the time indices of data to be randomized, the randomized series of precipitation, temperature, and radiation are $P_r = P_o\{I_p\}$, $T_r = T_o\{I_p\}$, $R_r = R_o\{I_p\}$, where I_p is a random sample from I, P_r, T_r, *and* R_r are the randomized series, and P_o, T_o, *and* R_o are the observed series of precipitation, temperature, and radiation respectively. In the second subcase the randomized series are $P_r = P_o\left\{I_p^1\right\}$, $T_r = T_o\left\{I_p^2\right\}$, *and* $R_r = R_o\left\{I_p^3\right\}$, where I_p^1, I_p^2, *and* I_p^3 are three different samples from I. In the first case, the autocorrelation of the three climate variables are destroyed, but their conditional probability distributions are preserved. In the second subcase, the autocorrelation in time and the cross correlations among precipitation, radiation, and temperature are destroyed. However, note that to maintain some realism in the input, the seasonal and diurnal cycles of the climatic input variables are retained. To achieve that the sampling pool is restricted for every variable based on the month and hour of the day is was observed.

3.2.2. Precipitation

The precipitation statistical structure is probably the most complex among the environmental drivers. The main features of the small-scale statistical structure of precipitation are its intermittent nature, highly skewed distribution, and autocorrelation [*Molini et al*., 2009; *Paschalis*, 2013; *Paschalis et al*., 2013, 2014a]. Event-scale precipitation structure affects the amount and timing of available water in the rooting zone. Moreover, due to lagged effects of the water flow within soil, the small-scale variability of precipitation can influence plant water availability over a much wider range of scales and potentially introduce long-term effects on ecosystem functioning [*Katul et al*., 2007a]. Evidence of such long-term effects has been provided by experimental studies for semiarid regions [*Swemmer et al*., 2007] and has been hypothesized to play a role in the Amazon rainforest [*Ivanov et al*., 2012].

In this study, four precipitation scenarios that encompass many plausible conditions are considered. In the first precipitation scenario (case 4 in Table 1), the correlation structure of precipitation is perturbed by randomizing the observed hourly precipitation, while preserving seasonal and diurnal patterns. The randomization of precipitation has two significant impacts on the precipitation statistical structure. First, precipitation autocorrelation in time is destroyed, and second, the distribution of coherent dry and wet spells is modified since precipitation clustering into storm events does not occur anymore. The altered precipitation has statistically shorter interstorm and intrastorm durations. To isolate the effect of the correlation structure of precipitation from amounts, the total precipitation annual amounts are set equal to the control scenario (i.e., the interannual variability of precipitation is preserved).

In the second precipitation scenario (case 5), interannual variability of precipitation is removed and precipitation series within year are standardized as

$$R_s^i(t) = R^i(t)\,\frac{\overline{R_a}}{R_a^i}\,, \tag{2}$$

where $R_s^i(t)$ is the standardized precipitation depth for time t of the year i, $R^i(t)$ is the recorded precipitation depth, R_a^i is the annual depth of the $i-$th year, and $\overline{R_a}$ is the long-term annual depth. This scenario allows the estimation of the sole impact of the small-scale structure of precipitation, which essentially remains intact, while the effects of the longer-term fluctuations are removed.

The third precipitation scenario (case 6) enhances precipitation peaks by employing the following probability transform:

$$R_s^+(t) = {F_g}^{-1}\left(F[R^+(t)], a_g, b_g\right) \tag{3}$$

where $R_s^+(t)$ is the positive part of the synthetic precipitation, $F[\cdot]$ is the cumulative distribution function of the positive part of the observed precipitation $R^+(t)$, and ${F_g}^{-1}[\cdot]$ is the inverse of the cumulative distribution function of the Gamma distribution with parameters a_g and b_g. The choice of such a cumulative distribution is

based on prior studies demonstrating that precipitation depths are reasonably approximated by a Gamma distribution [*Papalexiou et al.*, 2013; *Paschalis et al.*, 2014a]. The parameters a_g and b_g are estimated using the method of moments (the first two moments are used). The mean value is set to be the same as the observed precipitation, thereby preserving the amounts over long periods. The standard deviation is set to 4 times the observed value to amplify the peak magnitude. The synthetic precipitation time series has the same intermittency pattern as the observed, the same mean value but, as expected, larger peaks. This scenario is intended to reveal the potential of extreme high precipitation influencing the water and carbon fluxes, which has been previously found to be important especially in water limited ecosystems [*Knapp et al.*, 2008]. Similar to the first case, the annual totals of precipitation are standardized to preserve interannual variability.

The fourth precipitation scenario (case 7) unfolds the significance of the storm event precipitation depth. To separate the effect of the precipitation distribution within the event, and the potential influence of its peaks, synthetic precipitation series are constructed using the following integral

$$R_s(t) = \frac{1}{\Delta}\int_{t-\Delta/2}^{t+\Delta/2} R(t)\mathrm{d}t, \tag{4}$$

where $R(t)$ and $R_s(t)$are the observed and simulated precipitation depths, respectively. Choosing Δ comparable to a typical storm size, and smaller than the interstorm period, the resulting precipitation is structured in distinct precipitation events, with comparable cumulative precipitation depths and durations to the observed ones (per storm), but reduced peaks. For all sites, $\Delta = 12$ h is selected. This scenario reveals to what extent the precipitation amount of events rather than the subevent structure influence the functioning of the ecosystems [*Heisler-White et al.*, 2008]. In this case, the interannual variability of precipitation is also preserved.

3.2.3. Temperature

In contrast to precipitation, air temperature fluctuations are dominated by the two dominant modes, the seasonal and the diurnal, which explain much of the total air temperature variance. The rest of the variability consists of high-frequency fluctuations (hours to days) associated with weather patterns and low-frequency fluctuations (interannual and beyond) linked to phenomena such as the El-Niño Southern oscillation [*Gu and Adler*, 2011].

Temperature variability is investigated at the hourly and the interannual scales. For this reason, three different scenarios are constructed. In the first scenario (case 8), the correlation pattern of temperature at the hourly scale is altered: the series is randomized in the same fashion as for the precipitation case 4, preserving the diurnal and seasonal patterns as well as the marginal distribution of temperature. With this case, we explore whether persistence of temperature can alter ecosystem functioning. Moreover, the effect of the cross correlations of temperature with the rest of the climatic forcing is also investigated, since cross correlation is altered as well. To isolate the effect of the short-scale correlations, the mean annual temperatures are set equal to those of the observed series to preserve interannual variability consistent with the measurements.

In the second temperature scenario (case 9), interannual variability of temperature is removed using a procedure similar to equation (2). In this case, the effect of the intraannual variability of temperature is isolated by removing the effects of long-term variations found to be significant in temperature limited ecosystems [*Tian et al.*, 1998; *Babst et al.*, 2013].

Finally, a moving average filtering to the temperature series identical to equation (4) is implemented for the third temperature scenario (case 10). In this case, the distribution of the temperature is modified by smoothing warm and cold fluctuations occurring over short periods, while keeping the seasonal patterns of temperature unchanged. This case can reveal whether or not the probability density function of temperature significantly impacts water and carbon fluxes. Since the response of ecosystems to climatic forcing is, in general, nonlinear, any reduction in temperature extremes may have an impact, difficult to predict a priori, and is explored here. As before, interannual variability of temperature is also preserved.

3.2.4. Radiation

The last climatic variable to be investigated is incoming shortwave radiation at the land surface. The statistics of the radiation time series are similar to that of temperature, with the two major modes of variability being the seasonal and diurnal. Small-scale variability is linked to weather, with cloud formation reducing the

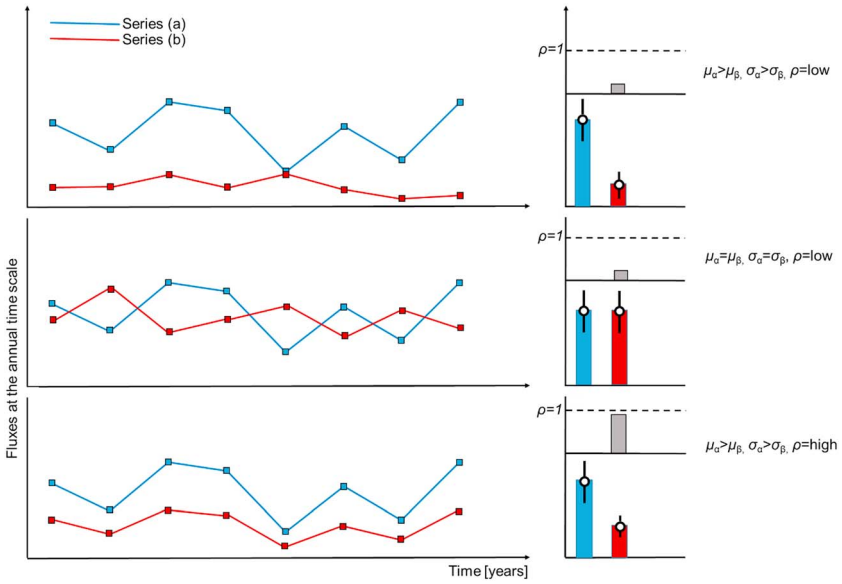

Figure 2. A schematic representation of the statistical evaluation presented in Figures 3 and 4: μ stands for mean value, σ is the standard deviation, and ρ is the correlation coefficient between series (a) and (b).

amount of direct radiation from its expected clear-sky value. Large-scale interannual variability is relatively low and can be associated with anthropogenic aerosol emissions and volcanic eruptions [*Wild et al*., 2005; *Norris and Wild*, 2007].

In the case of radiation, two different scenarios similar to the temperature cases are constructed. In the first one (case 11), the correlation structure is removed but the observed radiation interannual, seasonal, and daily variability are preserved; in the second radiation scenario (case 12), the interannual variability is removed.

3.3. Statistical Evaluation of the Simulations

The objective here is a systematic exploration of cross-scale information flow from small-scale climatic fluctuations to long-term carbon/water fluxes in various ecosystems. In particular, how short-term variability in precipitation, air temperature, and incident radiation translates to variability in water and carbon fluxes across temporal scales is explored.

3.3.1. Interannual Variability of Water and Carbon Fluxes

The effects of interannual and short-scale temporal variability of hydrometeorologic forcing on the "climatology" of ET and carbon assimilation are considered focusing on three aspects: (a) the mean values at the annual scale, (b) their variance, and (c) the "shape" of interannual fluxes, i.e., the temporal pattern of the multiyear fluctuations. A scheme of the analysis approach for water and carbon fluxes at the annual scale is presented in Figure 2. The three aspects are referenced to the control scenario, which uses the measured meteorological inputs. The evaluation of potential differences in the mean values and standard deviation for each scenario is presented (Figure 2). The correlation coefficient between annual time series of the control simulation and the time series obtained using the input scenarios is also investigated. This analysis provides a direct metric of the relative impact of the perturbed meteorological forcing statistics in modifying interannual variability of a given variable. In other words, given that each of the synthetic input scenarios alters only one property of the interannual or short-scale variability of the meteorological input, the impact of that specific property on the interannual variability of the water and carbon fluxes can be assessed as a reduced cross-correlation. The fluxes explored here are ET, the partition of ET into evaporation and transpiration, and gross primary production GPP. We chose to analyze GPP, representing the gross carbon assimilation, rather than net ecosystem exchange, which could be possibly a better descriptor of the total carbon balance of each ecosystem due to the large uncertainties involved in the simulation (and measurements) of ecosystem respiration components, especially those describing belowground heterotrophic respiration [*Vargas et al*., 2010].

3.3.2. Spectral Analysis

To quantify the influence of each of the investigated characteristics of climate variability on the modeled water and carbon fluxes across scales, the coherence spectrum between two time series is employed. The square coherence spectrum between two series $X(t)$ and $Y(t)$ is defined as

$$C_{xy}(f) = \frac{|S_{xy}(f)|^2}{S_{xx}(f)S_{yy}(f)}, \quad (5)$$

where f is the frequency, $S_{xy}(f)$ is the cross spectral density between the two series, and $S_{xx}(f)$ *and* $S_{yy}(f)$ are the spectral densities of $X(t)$ and $Y(t)$, respectively. The $C_{xy}(f)$ is bounded (i.e., [0, 1]). The coherence spectrum shows the similarity between X (t) and $Y(t)$ in the frequency domain. It is therefore a suitable technique to analyze signals across a wide range of temporal scales. The coherence spectra are estimated using the fast Fourier transform [*Press et al*., 1992; *Baldocchi et al*., 2000]. Post processing includes the use of a modified Welch's overlapped averaged periodogram method. All the calculations were performed in MATLAB. Alternative estimations, which are based on the wavelet decomposition, also exist and are gaining popularity in data analysis and model comparisons in ecological and climate studies but are not used here [*Torrence and Compo*, 1998; *Katul et al*., 2001; *Dietze et al*., 2011; *Stoy et al*., 2013].

Coherence spectra of simulated variables are computed using the control simulation ($X(t)$) and each of the 12 input scenarios ($Y(t)$). The frequencies at which coherence exhibits low values can be interpreted as the temporal scales in which the influence of the modified characteristic of forcing variability is significant. Due to the system nonlinearities and feedback between the processes controlling the water and carbon cycles, it is not expected that the impact of perturbations of meteorological inputs that are imposed at the highest frequency (1 h) will monotonically decrease with increasing temporal scales. The coherence spectra can be used as a tool to identify in which cases short-scale temporal variability of the meteorological forcing has the potential to affect water and carbon at larger scales, e.g., at the interannual level (section 3.3.1) and provide clues to a mechanistic explanation as to why such dependencies occur. A caveat related to the coherence spectra analysis is that an assessment of the "signal similarity" at low frequencies is highly impacted by the length of the analyzed series. For this reason the linear correlation analysis described before can serve as a complementary analysis to the coherence spectra.

The scales in the coherence spectral analyses considered span from 1 h (i.e., the frequency of the simulations) up to few months. Coherence estimates for coarser scales are unreliable due to the limited simulation length, which is restricted by the meteorological data availability for each site.

4. Results and Discussion

4.1. Presentation of the Results

The results of the two types of analyses are presented—the correlation analysis that is conceptually presented in Figure 2 and the squared coherence analysis that emphasizes information propagation across temporal scales from "forcing" (three climatic variables with various statistical structure) to "response" (mainly ET and GPP). Figures 3 and 4 present the outcome of the correlation analysis for each ecosystem, emphasizing the interannual variability of the fluxes, while Figures 5–8 suggest connections or interpretations between forcing and response variables specific to a given ecosystem and across seasons expanding on the results shown in Figures 3 and 4. Figure 9 summarizes the outcome of the squared coherence analysis across sites and by response variable. Additional information that yield outcomes similar to the ones in the aforementioned figures are only included in the supporting information. For clarity, we report only the first subcase of the perturbation 3 (Table 1) in all figures. In this subcase, precipitation, temperature, and radiation were randomized using the same time index, i.e., preserving the covariance (section 3.2.1). For all fluxes and stations considered, there was not substantial difference between the two subcases indicating that destroying the conditional probability distributions between precipitation, temperature, and radiation does not add much to the alteration of their autocorrelations. For completeness, results from the second subcase are reported in the supporting information.

4.2. Water-Limited Ecosystem (Lucky Hills)

Lucky Hills site represents a water-limited ecosystem. The mean values of ET at the annual time scales are almost equal for all input scenarios (Figure 3a). These findings are consistent with expectations as

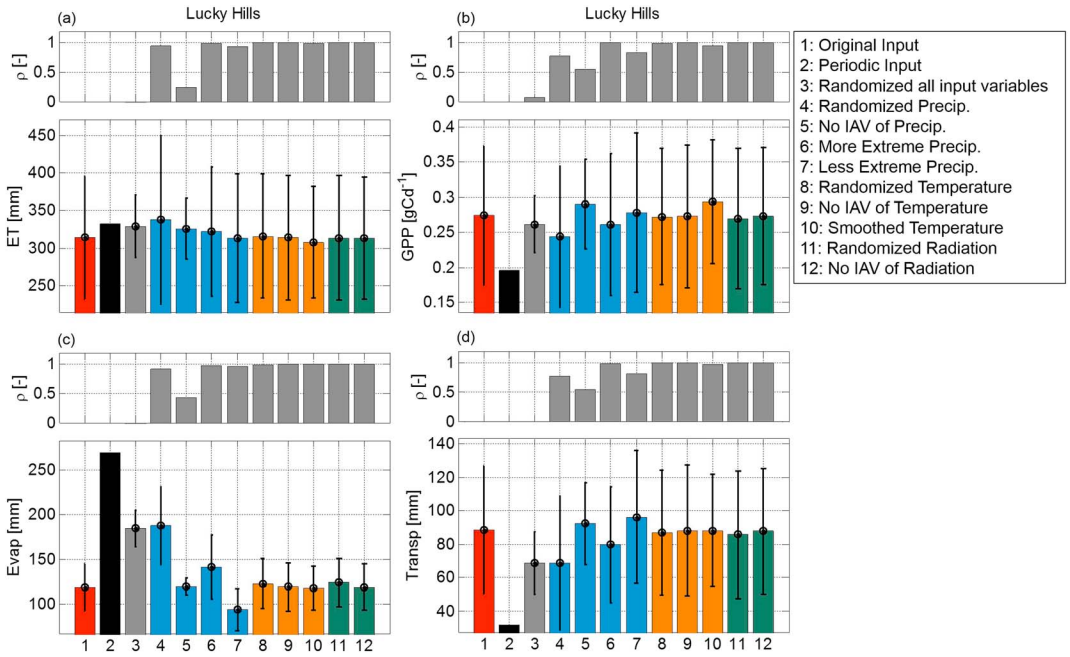

Figure 3. Interannual statistics for the Lucky Hills station for (a) evapotranspiration, (b) gross primary production of the evergreen shrubs (creosote bush), (c) evaporation, and (d) transpiration of the evergreen shrubs. The lower part of each panel shows the mean value (bars) and the standard deviation (error bars) for the 12 different meteorological input scenarios. Input scenarios related to perturbing precipitation only are marked as blue, input scenarios related to perturbing temperature only are shown in yellow, and input scenarios related to perturbing radiation only are shown in green. The upper part of each panel shows the correlation coefficient between the output of each scenario for a given variable at the annual scale, and the output of the simulation of the control scenario (1). Correlation values $\rho[-]$ are shown for the cases (3–12). For case the 1, it is trivial that $\rho = 1$.

the site is located in the water-limited regime where potential evapotranspiration PET $>$ ET $\approx P$ [*Fatichi and Ivanov*, 2014] according to the Budyko's curve. Water losses due to surface runoff and leakage to the deep soil layers are small for this location (≈2–20 mm yr^{-1}). This fact explains the reason why the basic determinant of the shape of interannual fluctuations of ET is the total annual precipitation depth. This finding is further illustrated by the low value of the correlation coefficient between the annual fluxes of ET estimated for the control scenario and the case 5 with no interannual variability (IAV) of annual precipitation (Figure 3a).

Although precipitation variability does not influence the total annual ET flux, it affects the partitioning between evaporation and transpiration (Figures 3c and 3d). Both the total amount of annual precipitation and precipitation structure at short temporal scales impact the partition between ground evaporation and transpiration because precipitation intensity affects interception and soil moisture vertical distribution. This has a net effect on the composition of the ET flux.

Scenarios that impose a loss in the internal correlation and intermittency structure of precipitation (Figure 3c, cases 3 and 4) or a periodic input (Figure 3c, case 2) lead to increased evaporation from interception and bare soil evaporation losses. The reason for larger evaporation from interception is that when precipitation events are not sufficiently large (cases 2–4), higher amounts of water are intercepted by the canopy. The reason for enhanced bare soil evaporation is deemed to be related to how precipitation wets the soil column. For water to penetrate deeper into the soil and become available for root uptake, large precipitation pulses are required. In the absence of well-structured precipitation events (i.e., precipitation events that last long to accumulate a significant amount of water), infiltrated water is mostly in the top soil layer and dissipated mostly as evaporation from the soil surface.

The way precipitation structure determines water availability in the root zone subsequently affects root access to water, and thus transpiration. As shown in Figure 3d (cases 2–4), when evaporation becomes the dominant flux, less water is available for plant uptake and transpiration. Total precipitation and precipitation

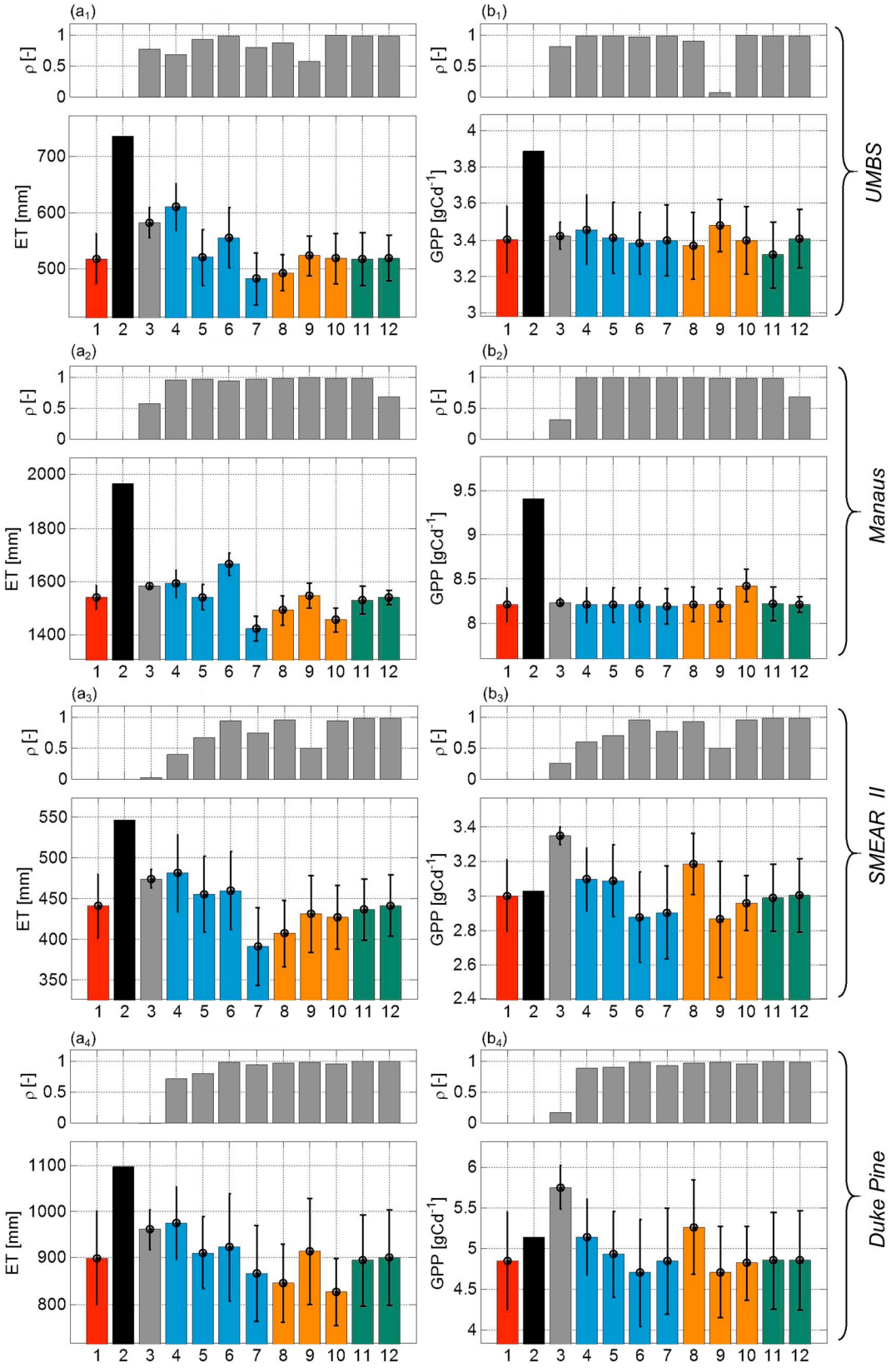

Figure 4. Same as Figure 3 but for the other sites. In this figure only the panels of (a) evapotranspiration and (b) gross primary production are shown. Subscripts 1–4 refer to the (1) UMBS, (2) Manaus, (3) SMEAR II, and (4) Duke Forest sites, respectively.

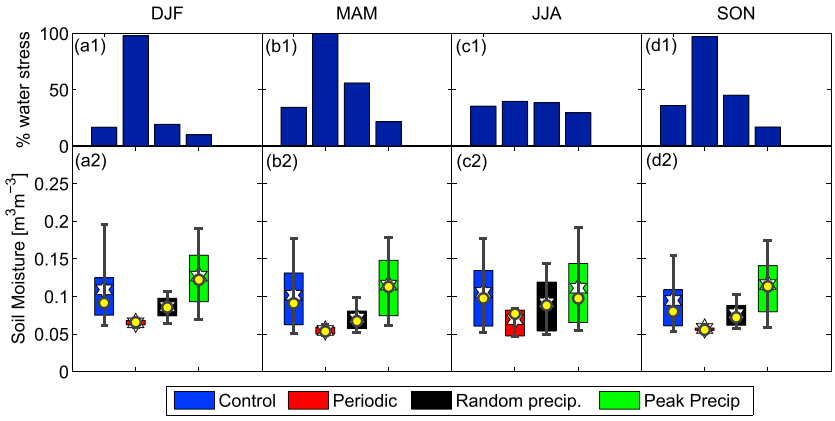

Figure 5. Analysis of the plant water stress for the Lucky Hills site (see section 4.2). The four panels represent the four seasons. The upper plots (a1, b1, c1, and d1) show the percentage of time vegetation is under water stress for the four different precipitation input scenarios (cases 1, 2, 4, and 6 in Figure 3). The lower plots (a2, b2, c2, and d2) show a box plot of the soil moisture integrated in the root zone. Boxes represent the 25%–75% percentiles, bars the 10%–90% percentiles, circles show the mean value, and stars show the median value.

structure are significant for determining transpiration at the annual scale, as shown by the low values of the correlation coefficient between precipitation and transpiration in Figure 3d (cases 2–4).

The way precipitation structure at the short temporal scales affects the partition of *ET* into its components has been found to be similar in terms of patterns across all ecosystems analyzed. For this reason, the partition discussed in detail for the case of Lucky Hills is not further repeated in later sections. A detailed quantification of this effect is given in the supporting information.

Annual total and precipitation structure at the finest temporal scales have also a major influence on carbon assimilation. Due to the linkage between photosynthesis and transpiration through stomatal conductance, the behavior of interannual variability of GPP is similar to that of transpiration (Figure 3b). Short-scale variability of precipitation affects root zone water content, and specifically, the time fraction that vegetation is under water-stress (Figure 5) defined here as the percentage of time during which the integrated soil water content in the root zone is below the water content threshold at which stomata begin to close. Similar to transpiration, carbon assimilation is lower whenever the soil water conditions are not favorable for vegetation over longer periods. For the semiarid location of Lucky Hills, this occurs when either the intermittent nature of precipitation is not taken into account (i.e., input scenario with periodic precipitation) or whenever discrete precipitation events (i.e., input scenario with no correlation structure) cannot wet the root zone sufficiently deep (Figure 3b, cases 2–4). This result is also consistent with previous modeling studies, which showed a significant dependence between the storm arrival rates, the event precipitation depths, and vegetation productivity [*Ridolfi et al.*, 2000; *Daly et al.*, 2004; *Porporato et al.*, 2004].

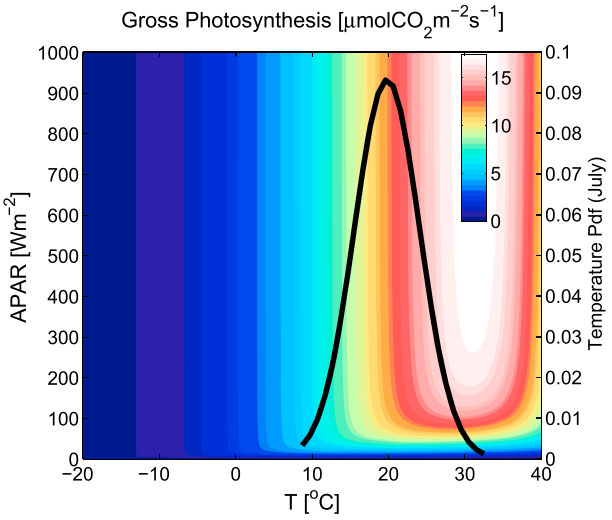

Figure 6. Response gross photosynthesis (A_g) to absorbed photosynthetic active radiation and leaf temperature (T) as estimated by the model. The contours show A_g according to the color bar. The photosynthesis biochemical parameters are the same as the parametrization of the *PFT* representing the deciduous forest in UMBS, and for this plot a relative humidity $U = 0.8$ and an atmospheric CO_2 concentration of 380 ppm were considered. The thick black line shows a normal fit of the probability density function of hourly air temperatures during July in UMBS (see section 4.3).

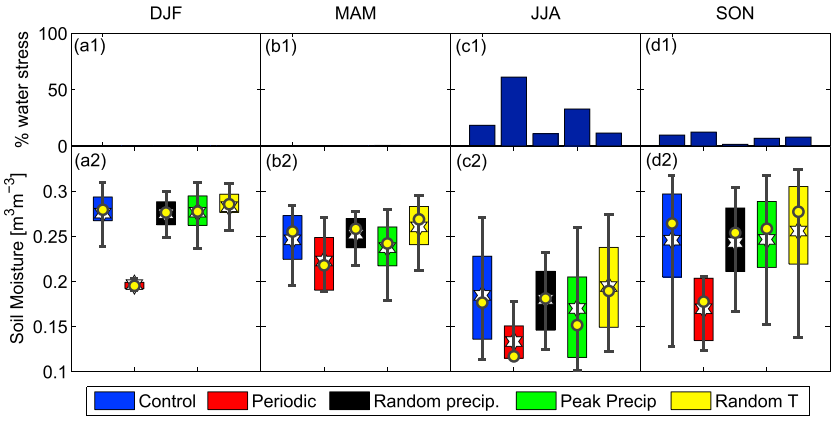

Figure 7. Same as Figure 5 but for the SMEAR II site (see section 4.5). The scenarios shown are the control scenario (blue, case 1), the scenario with periodic input (red, case 2), the scenario with randomized precipitation at the highest frequency (black, case 4), the scenario where precipitation peaks are enhanced (green, case 6), and the scenario where temperature is randomized at the higher frequency (yellow, case 8).

An interesting feedback is the increase in leaf area index (LAI) due to enhanced GPP, which can then lead to potential reductions in soil moisture. Enhanced GPP can lead to increased LAI, which in turn increases water loss from interception (due to larger interception capacity) and transpiration, thus creating less favorable soil water conditions for the plant. This feedback is generally captured by the model but when it operates at longer multiyear scales, longer-term simulations and an explicit accounting of nutrient dynamics should be carried out, which is not the case of this study.

How the short-temporal-scale perturbations in the precipitation time series affects the behavior of water and carbon fluxes across a range of temporal scales, and how they impact ecosystem performance at the annual scale, is considered for the Lucky Hills site by analyzing the coherence spectra. The first feature concerning the spectral analysis is the substantial difference of the shape of the coherence spectra corresponding to the randomization of precipitation, temperature, or radiation. The effect of the distortion of the short-scale variability of radiation and temperature, in general, seems to decrease with increasing scale, as illustrated by the increasing value of the squared coherence with decreasing frequencies (Figures 9c–9f). In contrast, the distortion of precipitation structure at the highest frequency affects the behavior of the water and carbon fluxes also at lower frequencies. The explanation for this behavior is that radiation and temperature affect immediately (i.e., at the same time scale) the biochemical processes related to photosynthesis and the biophysical process of evapotranspiration. Conversely, precipitation structure at the finest scale can alter the availability of water in the root zone, which impacts transpiration and GPP. The movement of water in

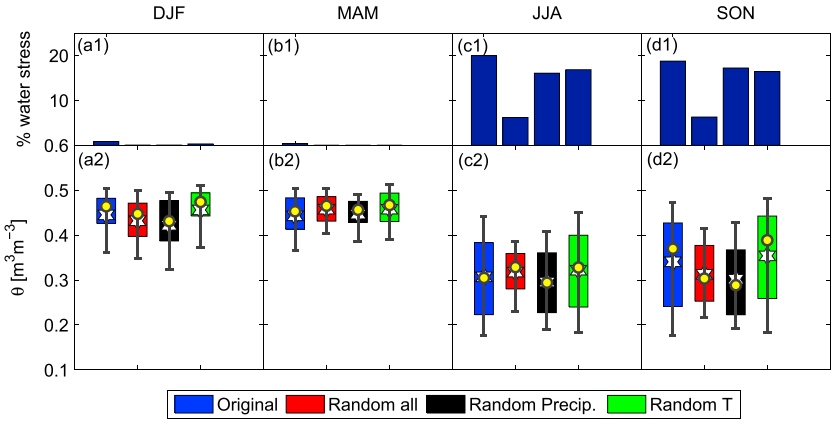

Figure 8. Same as Figure 5 but for the pine plantation in Duke Forest (see section 4.6). The scenarios shown are the control scenario (blue, case 1); the scenario with randomized precipitation, temperature, and radiation at the highest frequency (red, case 2); the scenario with randomized precipitation (black, case 4); and temperature (green, case 8) at the highest frequency.

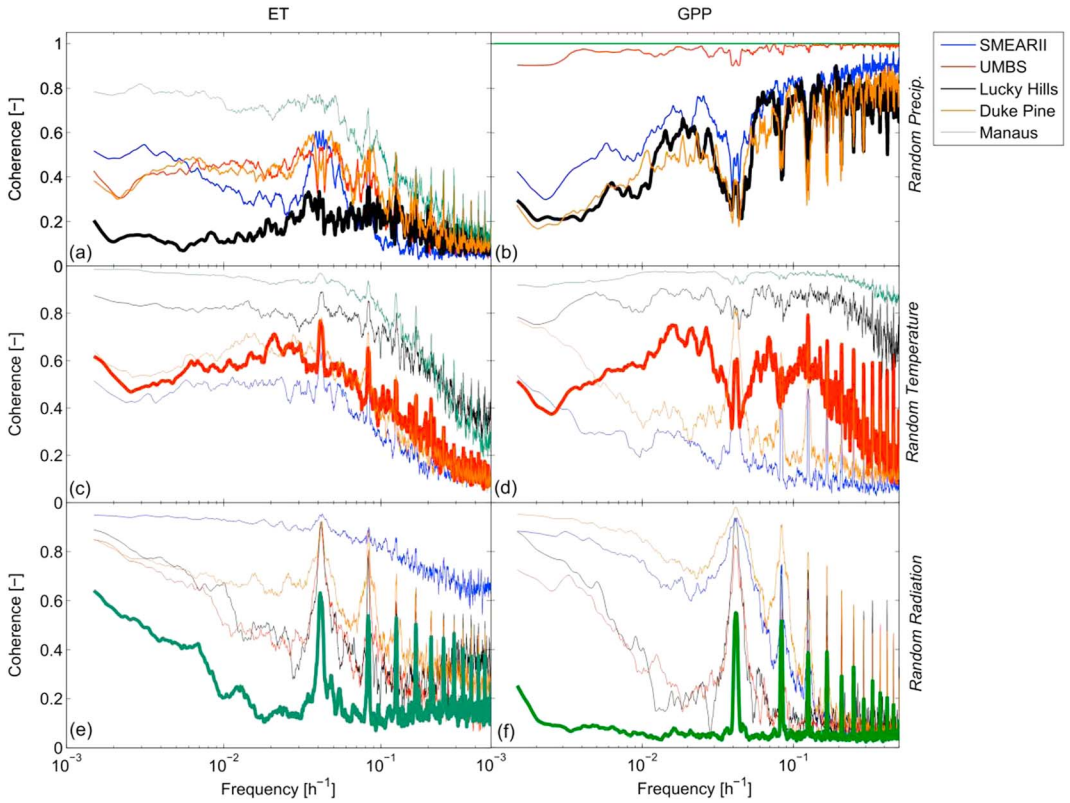

Figure 9. Squared coherence spectra between the simulated time series of (a, c, and d) ET and (b, d, and f) *GPP* between the control scenario and the synthetic input scenarios that randomize precipitation (Figures 9a and 9b), temperature (Figures 9c and 9d), and incoming radiation (Figures 9e and 9f) at the highest frequency (1 h^{-1}). For each panel, the atmospheric variable of interest, which is the most important limiting factor for the ecosystem functioning, is marked as a bold line.

the soil profile has a much longer characteristic time scale (approximately days) in comparison to the imposed distortions at the short time scale by the precipitation structure (hours) [*Katul et al*., 2007a; *Nakai et al*., 2014]. For this reason, lower squared coherences occur at lower frequencies despite that the distortion is only introduced at the highest frequencies. This remarks the potential of the short-scale variability of precipitation to impact the behavior of carbon and water fluxes at much longer time scales. Temperature and radiation, both in terms of annual means and short-scale temporal structure, play only a minor role on the ecosystem functioning since they rarely represent limiting factors.

The findings presented here provide mechanistic explanations of the importance of precipitation pulse structure (amounts, organization, and recurrence) for ecosystem functioning, which has been empirically observed in many semiarid and desert ecosystems [*Noy-Meir*, 1973; *Huxman et al*., 2004b; *Loik et al*., 2004; *Nagler et al*., 2007; *Williams et al*., 2009].

4.3. Temperature-Limited Ecosystem (UMBS)

The second ecosystem investigated here is the deciduous forest located near the University of Michigan Biological Station. The ecosystem is hypothesized to be primarily limited by low air temperature and, to a smaller degree, by water and radiation.

ET at the annual time scale is primarily influenced by the short-scale variability in precipitation and, to a less extent, by the temperature variability (Figure 4a1, all cases). The shape of the IAV of ET, expressed as the loss of correlation between the output of the control simulation and the simulations with the considered scenarios, is influenced both by precipitation and temperature variability. Specifically, the differences in the magnitude of ET at the annual time scale, which are as high as 20% (Figure 4a1, cases 3–12), are primarily driven by the abiotic process of evaporation of water intercepted by the canopy and bare soil evaporation (see the supporting information). Since UMBS is not in a water-limiting regime (based on the Budyko curve),

ET is not strictly limited by the total amount of annual precipitation (e.g., no loss of correlation for case 5). However, ET can be sensitive to precipitation variability. The mechanisms that impact ET at the annual time scale are due to precipitation interception by canopy and bare soil evaporation from the upper soil layer. The input scenarios leading to enhanced evaporation from soil and canopy are the ones where precipitation is not structured in distinct events (Figure 4a1, cases 2–4). Since soil water availability is limiting vegetation at the UMBS only rarely, changes in transpiration flux have a minor influence on ET (supporting information).

The mean annual gross primary production is essentially identical for all the forcing scenarios with the exception of one where variability in all of the input types of forcing is neglected (Figure 4b1, case 2). In particular, the loss of temperature variability at the shortest scale enhances annual GPP (Figure 4b1, case 2). The reason for this GPP enhancement is the nonlinear response of photosynthesis to leaf temperature, where photosynthesis is defined here as the gross assimilation of carbon per unit leaf area [*Wohlfahrt and Gu*, 2015] (Figure 6). Photosynthesis has a steep increase with increasing temperature at low leaf temperatures and reaches a plateau around the optimal temperature for carbon assimilation. Furthermore, the temperature distribution at UMBS lies between the steep response regime and the plateau. This implies that time averaging (indicated by the overline) results in $\overline{\mathrm{GPP}(T_s)} < \mathrm{GPP}(\overline{T_s})$. At the UMBS, this inequality is often satisfied during summer when productivity is maximum, and removing cold spells (as done in case 2) results in a considerable enhancement of GPP. The contributions of precipitation and radiation variability are negligible.

The shape of the IAV of GPP is almost uniquely determined by the mean annual temperature (Figure 4b1, case 9). Standardization of the annual fluxes in terms of temperature leads to a complete loss of correlation between the annual fluxes of GPP of the control and synthetic input scenarios (case 9). Using the mean growing season temperature, rather than the mean annual temperature, a more appropriate choice since the UMBS forest is deciduous does not affect the finding, since the mean annual and the mean growing season temperature are highly correlated (not shown here). Short–temporal-scale variability of temperature at the UMBS is unlikely to influence the annual behavior of carbon fluxes since it does not result in long-lasting effects (i.e., no information transfer from small to large scales). Temperature variability at the shortest temporal scale mostly affects the biochemical processes of photosynthesis that operate at the same scale. This does not influence processes with long memory (i.e., temperature effects are not "stored" in the system); thus, the impact of hourly temperature variability to the variability of GPP across scales decreases rapidly with increasing temporal scale. An illustrated signature of this finding is the increased squared coherence between GPP of the control input (case 1) and the random input (case 8) at lower frequencies (Figure 9d). Temperature effects could potentially be stored in the ecosystem, if plant reproduction would be considered (e.g., carbon assimilation affected by temperature in 1 year may influence the survival of the following offspring). However, since reproduction is neglected in present paper, further discussion is not provided.

4.4. Radiation-Limited Ecosystem (Manaus)

The tropical rainforest located close to Manaus is an ecosystem expected to be primarily limited by radiation availability, given the high temperatures throughout the year, the high precipitation, and the longer root system that gives access to deep soil water (with the assumed root depth equal to 10 m). The mean annual ET losses in Manaus are affected by the short-scale temporal variability of precipitation and temperature, but not by radiation (no change in annual magnitude for cases 11 and 12). Similar to the UMBS site, the loss of short-scale correlation in the forcing series leading to unstructured rainfall without distinct storms (Figure 4a2, cases 2–4) results in higher ET, primarily due to abiotic contributions (see the supporting information). The reduction of precipitation peaks lead to higher ET due to the higher amount of water intercepted by the canopy that can evaporate before reaching the ground. This effect is more pronounced at this site due to the relatively high leaf area index (i.e., higher interception capacity) and the yearlong growing season, which both imply higher evaporation from interception storage, when compared to the other sites. Even though precipitation and temperature variability can influence the mean annual ET, they have no impact on the shape of the IAV of ET. In other words, differences in the short-scale precipitation or temperature structure can shift the time series of the annual fluxes of ET without changing its shape.

Short-scale temporal variability of radiation has no appreciable effect on the IAV of ET. However, the mean annual incoming radiation affects the shape of the IAV of ET. This is illustrated by the loss of correlation

between annual fluxes of ET as modeled for the control scenario and input scenarios in which the IAV of incoming radiation is suppressed (Figure 4a2, case 12).

The mean values of GPP are similar for all the input scenarios, except the scenario in which variability of all of the meteorological parameters is neglected. In this case, GPP is enhanced (~14%). The reason for this enhancement of GPP is similar to the one for the UMBS case related to temperature, but in this case with radiation being the more limiting hydrometeorological variable. Photosynthesis is affected in a nonlinear manner by incoming shortwave radiation and in particular by PAR (photosynthetically active radiation over 400–700 nm wavelength range). In tropical rainforests, overcast conditions occurring during wet seasons can substantially limit photosynthesis. The dynamic effects of cloudiness cannot be captured when radiation variability at the hourly scale is neglected (Figure 4b2, case 2). Furthermore, due to the concave nonlinearity of the response of photosynthesis to incident PAR, it follows that $\overline{\mathrm{GPP}(\mathrm{PAR})} < \mathrm{GPP}\left(\overline{\mathrm{PAR}}\right)$ [see also *Medvigy et al.*, 2010].

Similar to ET, the shape of the IAV of GPP is solely influenced by the mean annual magnitude of incoming radiation. This influence is best illustrated by a low correlation coefficient between the annual fluxes of GPP of the control scenario and the input scenario in which interannual variability of incoming radiation is neglected (Figure 4b2, case 12). Short-temporal-scale variability has no appreciable influence on the large-temporal-scale fluctuations in carbon assimilation. The reason is that radiation influences photosynthesis almost immediately at short scales and no residual contribution of such short-scale radiation variability is retained at long time scales. In other words, there is no considerable long-term "storage" of the radiation effects in this ecosystem, for instance through changes in leaf area index (that is close to maximum here), forest structure, and composition (which are assumed static), or transpiration that would affect soil moisture. The short-scale discrepancies of GPP introduced through the short-scale distortions in the radiation series cannot propagate to larger temporal scales such as the IAV. An indication of the reduction of influence of the short-scale radiation variability on carbon and water fluxes is the nearly monotonic increase of coherence with scale between the time series of GPP of the control case and of the synthetic case 11 (Figures 9e and 9f). Due to the short range of frequencies for which the coherence can be estimated (due to the limited amount of input data; Figure 9), we cannot compute the behavior of coherence up to the annual scale.

4.5. Colimited Ecosystem (SMEAR II)

The boreal forest in Finland is limited by two main environmental factors: low temperatures and relatively low precipitation. Boreal forests are also known to be nitrogen limited, but this limitation is outside the scope of this study. The nitrogen limitation effects are partially accounted for in the sensitivity of the maximum carboxylation capacity to temperature. However, the IAV of the nitrogen cycle is not considered.

ET fluxes at the annual scale are influenced by the short-scale variability of precipitation and temperature but are almost insensitive to radiation variability (no change in annual magnitude for cases 11 and 12), even though the site is located at a high latitude and thus radiation is theoretically a limiting resource for ecosystem functioning. Similar to the sites considered previously, input scenarios that disrupt precipitation structure, and especially its organization into distinct storm events, generally lead to the enhanced ET fluxes, primarily due to abiotic contributions (Figure 4a3). Further, a loss of correlation of the temperature at the hourly time scale leads to a small decrease in ET. Notably, in terms of variability of ET fluxes at the annual scale, most of the features of variability of precipitation and temperature contribute to the shape of IAV of ET, as illustrated by the low correlation coefficients between the control simulation and scenarios 3–10 (Figure 4a3). The most important features of precipitation forcing are its correlation structure, its distribution —with emphasis on peaks, and the magnitude of annual precipitation. In terms of temperature, the annual temperature and, to a smaller degree, the temperature correlation structure at the fine temporal scales play a role in ecosystem ET. This result illustrates that the predictive power of relations linking annual temperatures or annual precipitation to the IAV of ET will perform very poorly for this site.

Carbon assimilation is also affected by both precipitation and temperature variability. In terms of mean values, the loss of correlation structure of precipitation or temperature leads to a small increase in GPP (up to 10%, case 3). Conversely, a decrease or an increase in precipitation peaks leads to a small reduction in GPP. The reason for these responses is that the short-scale temporal variability of precipitation and temperature can influence soil water balance, and since water availability may be limiting at this site, it can affect the duration during which vegetation is under water stress (particularly during summer; Figure 7). The results

from this site support the notion that the effects of short-scale variability in precipitation and temperature can propagate across scales and influence the IAV of water and carbon fluxes, but only if mediated through a storage term (e.g., through the water availability in the root zone).

4.6. Nonlimited Ecosystem (Duke Forest Sites)

A deciduous hardwood and an evergreen pine forests co-located within the Duke Forest are studied in the last analysis. For clarity, only the results for pine stand are presented due to their similarities with the hardwood forest. Detailed results for the hardwood forest can be found in the supporting information. Temperatures in the Duke Forest are reasonably high, such that they do not hamper photosynthesis substantially during periods of leaf presence, and frost occurrence is rare. Precipitation is sufficient to satisfy plant demand, with the exception of few intense but rare drought events [*Palmroth et al*., 2005]. Because of this, we characterize the system as "nonlimited." In Duke Forest, vegetation has been found to be mostly nitrogen limited [*Oren et al*., 2001; *Palmroth et al*., 2013], but since T&C does not simulate soil biogeochemistry and nitrogen cycles, we cannot currently investigate the effect of this limitation.

The mean annual ET of the Duke Forest is sensitive to both precipitation and air temperature variability. In general, as was the case with the ecosystems considered previously, whenever precipitation is not well structured into distinct events, bare soil evaporation and evaporation of intercepted water from the canopy can substantially increase the total ET (Figure 4a4, cases 2–4). The most important feature is that the loss of correlation of ET fluxes at the annual scale between the control simulation and the rest of the scenarios is generally small. This finding suggests that meteorological variability at the hourly or annual scale only marginally influences the shape of the IAV of annual ET losses. In other word, the large-scale characteristics that are preserved throughout all the simulations, such as the vegetation phenology, are the major determinants of the shape of the IAV. The only cases in which there is some loss of correlation is when the IAV of precipitation is neglected or when the short-scale precipitation structure is destroyed. In those cases, the correlation coefficient can drop to ~0.7.

Similar to the annual ET fluxes, the mean GPP fluxes at the annual time scale are affected by both the variability of precipitation and air temperature, even though the shape of IAV of these fluxes is substantially unaffected (note the high correlation coefficient in Figure 4b4). In general, differences in the magnitude of the mean value of GPP are below 10%. A common behavior in both the pine and the hardwood stands is that disabling correlation, both in terms of precipitation (Figure 4b, case 3) and temperature (Figure 4b, case 8), leads to higher GPP. When a loss of correlation at the fine temporal scale for both variables is imposed, the results provide the highest carbon assimilation. The reason for this small enhancement of GPP is that the loss of correlation structure of precipitation and/or temperature at the highest frequencies tends to reduce the period during which the ecosystem is water-stressed (Figure 8). Even though this time difference is small, it occurs during the most productive period of the year and thus translates to a nonnegligible difference in carbon assimilation.

4.7. Synthesis

The common mechanisms and their related physical processes linking the hydrometeorological temporal variability to the variability in water and carbon fluxes and how short-term information propagates to longer scales are summarized in the following. A schematic representation of the relevant mechanisms is presented in Figure 10. Variability in precipitation, temperature, and radiation can have either a direct or an indirect effect on (a) the rate of water infiltration in the soil, (b) the biochemistry of carbon assimilation, and (c) the partition of net radiation into sensible and latent heat components.

Precipitation variability, and in particular its structure in well-organized events, affects directly the partition of water into interception, near-surface soil water storage, deep-soil water storage, and runoff. In general, precipitation organized in concentrated events leads to low interception by the canopy and a strong percolation of water to deeper soil layers. Further, a large precipitation depth or intense precipitation in a single event may lead to surface runoff. These differences in water partition among the various water storage compartments subsequently (and indirectly) affect the partition of net radiation into sensible and latent heat fluxes. Whenever a larger amount of water is available at either the canopy surface or in the upper soil layer, the abiotic components of evaporation (e.g., soil evaporation and evaporation from interception) are enhanced. This can lead to a lower water availability in deeper soil and thus in the root zone. Water limitations in the root

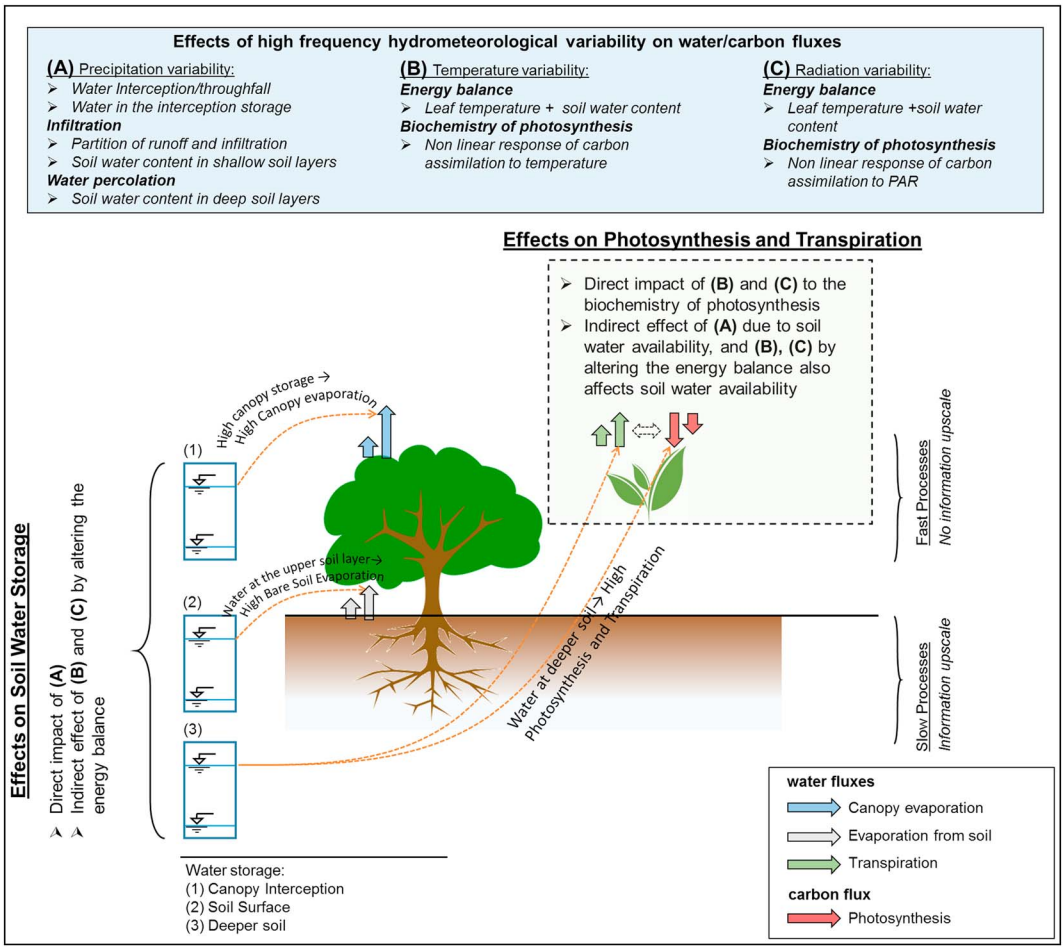

Figure 10. A schematic representation of the physical mechanisms explaining the effect of high-frequency hydrometeorological variability on water/carbon fluxes and transfer of variability across temporal scales.

zone may inhibit vegetation productivity and transpiration due to stomatal closure. The direct effect of the water flux partitioning and the indirect effect on the energy balance occur at all of the sites, while the indirect effect leading to vegetation productivity inhibition occurs only at the water limited sites, where the soil water potential can drop below the stress threshold level.

Temperature and radiation variability can affect directly the biochemistry and the energy balance of the ecosystem and have the potential to indirectly affect the soil water availability. Leaf/canopy photosynthesis depends nonlinearly on both leaf temperature and absorbed photosynthetic active radiation. Due to this reason, the distribution, rather than the correlation properties of temperature and radiation, affect carbon assimilation. The lack of importance of the correlation structure is due to the fact that photosynthesis is a fast process (i.e., responding in the order of few minutes to temperature and radiation forcing), and thus, it does not carry memory effects. In our study, modifying temperature or radiation distributions had an influence only for the sites where either temperature or radiation were limiting vegetation productivity (temperature for UMBS and SMEAR II; radiation for Manaus). The statistical distribution of temperature and radiation (e.g., concentration in heat/cold waves and diurnal variability) modifies the relative contributions of latent and sensible heat fluxes, and thus evaporation, transpiration, and the distribution of leaf temperature. Such an impact has the potential to modify the soil water availability and its vertical distribution in the soil profile, potentially affecting root water uptake and vegetation productivity. This indirect influence of temperature and radiation on soil water affects subsequently carbon assimilation only if it translates into periods of low soil water moisture, and thus plant water stress. This was featured when water and temperature were simultaneously a limiting factor (SMEAR II).

Given the relatively short time span of the simulation period, we did not investigate the dynamics of nutrient limitations, species composition, forest demography (time scale approximately years). However, these are additional low-frequency processes, which could potentially propagate information at even longer time scales.

4.8. Study Limitations and Perspectives

The numerical analysis provided here has limitations that need to be discussed and form open questions for future research.

First of all, the results are based on model simulations only, which have inherent assumptions and depend on the model structure. Perhaps the most important limitation of the current generation of ecohydrological and global dynamic vegetation models is the lack of a commonly accepted mechanistic representation of vegetation growth and stress, mineral nutrition, and long-term forest demography (mortality, recruitment, and seedling survival) [*Moorcroft*, 2006; *Fisher et al*., 2010; *Pappas et al*., 2013; *Xu et al*., 2013; *Fatichi et al*., 2014b; *Körner*, 2015]. As a result, large discrepancies have been identified in a number of model intercomparison projects [*Dietze et al*., 2011; *McDowell et al*., 2013; *Stoy et al*., 2013]. T&C has been found to reproduce well carbon and water fluxes across temporal scales for many ecosystems (including those considered in this study). However, interpretations should be considered with necessary caution. The most important components of ecosystem functioning that are not handled in T&C are (1) detailed soil biochemistry/plant mineral nutrition, (2) root adaptations to water and mineral resource limitations, (3) internal plant hydraulics, (4) forest demography, and (5) hydraulic redistribution. The first component can potentially provide additional limitations to plant growth and carbon assimilation. One should note that it also represents a poorly constrained component in carbon cycle modeling [*Todd-Brown et al*., 2014]. The second component could add a further restriction in the interpretation of the results, given that the time scales of root adjustments are comparable with the simulation length [*Joslin et al*., 2000; *Yuan and Chen*, 2010]. The third component may be important for regulating subdaily stomatal conductance and water stress but its importance decreases for longer temporal scales [*Bohrer et al*., 2005]. The forth component is typically relevant for time scales larger than ~20 years but could possibly reflect on our results since during a "good year," plants can invest excess carbon to enhanced reproduction, affecting the survival rates of the next offspring, and thus add an additional influence to the ecosystem functioning [*Peters*, 2000; *Reichmann et al*., 2013]. Additionally, during a "bad" year, increased mortality can also affect the ecosystem dynamics with long-lasting effects. The last component is receiving significant attention across a wide range of ecosystems (grasses to plantation forestry) and climates (temperate, mesic, and arid), as reviewed elsewhere [*Caldwell and Richards*, 1986; *Mendel et al*., 2002; *Amenu and Kumar*, 2008; *Siqueira et al*., 2009; *Neumann and Cardon*, 2012; *Volpe et al*., 2013; *Manoli et al*., 2014], but its significance at the ecosystem scale is hard to establish because of limited observations.

Second, the input scenarios for this analysis correspond to synthetic cases in which input variables have been constructed to preserve specific statistical characteristics. The choices were dictated by the goal of investigating individual aspects such as short term or IAV of precipitation, temperature, and radiation without confounding effects. In this sense, the constructed scenarios cannot strictly correspond to realistic observable cases but are rather intended to provide results concerning ecosystem functioning that can be unfolded from natural variability in hydrometeorological forcing. Frameworks for generating more realistic hydrometeorological forcing exist and rely on stochastic weather generators [*Fatichi et al*., 2011; *Paschalis et al*., 2013] that can also be tuned to reproduce the findings of the latest climate research, integrating also the effect of anthropogenic CO_2 emissions.

Finally, while diverse in vegetation type and climatic conditions, the number of ecosystems considered here is limited and falls short of providing a general picture of all ecosystem functions. To assess the global effect of short-term climatic variability on water and carbon fluxes worldwide, a similar framework can be replicated in a global model or calibrating the model in the entire data set of observation networks such as FLUXNET [*Wilson et al*., 2002; *Bonan et al*., 2012].

5. Conclusions

The effect of short temporal scale (hourly scale) and interannual variability of precipitation, temperature, and radiation on the water and carbon fluxes for six ecosystems representing a range of hydrometeorologic conditions has been explored. Numerical experiments were constructed in which one key feature of the

variability of the three major meteorological variables was perturbed or statistically distorted from its observational (or reference) record. Subsequently, a state-of-the-science mechanistic ecohydrological model was used as a process-based "filter" to link each of the perturbed climatic variables to ecosystem performance in terms of water and carbon fluxes. Based on the results of these simulations, the effects of each distinct feature of the meteorological variability were analyzed. In particular, we focused on the interannual variability of ET and GPP. With aid of spectral analysis, we highlighted the manner in which small-scale temporal variability of hydrometeorological input propagates across scales to alter the ecosystem response in terms of water and carbon cycles.

The most significant result is that short-scale variability of hydrometeorological forcing can impact carbon and water fluxes across a range of temporal scales, being primarily linked to the main resource limiting a given ecosystem. In particular, following are the conclusions:

1. Precipitation structure at the fine temporal scales and, specifically, its intermittency impacts the interannual variability of ET across all sites. Whenever water is not a strong limiting factor, significant effects on annual ET magnitude occur due to changes in various statistical components of the precipitation structure. Further, these changes cause significant impact on ET partition between evaporation and transpiration across all the sites, with the influence of abiotic processes playing the major role. This result demonstrates the fundamental role of the so-called "pulse structure" of precipitation and illustrates its importance across all ecosystems, not necessarily constrained to water-limited regimes.
2. Temperature variability can affect water and carbon fluxes only in ecosystems where temperature is a major limiting factor for the leaf-level biochemical processes, thus affecting carbon assimilation. Since photosynthesis responds at the same time scale as fine-scale fluctuations of temperature, short-scale variability in temperature can affect the total annual carbon assimilation, but the long-scale fluctuations of carbon fluxes (expressed in this study as the shape of interannual fluxes of GPP) are primarily affected by the long-scale fluctuations of temperature (e.g., its interannual variability). Short-scale temporal variability of air temperature can affect the shape of interannual fluxes of GPP only if it can affect the root zone soil water availability and increase or decrease the duration of water-stress periods. This occurs when colimitation of water and temperature takes place.
3. Radiation variability can affect water and carbon fluxes in a similar manner to temperature. Radiation affects evaporation, transpiration, and photosynthesis at the highest-frequency regime, and for this reason, radiation variability at the shortest scale does not influence the low-frequency responses of water and carbon fluxes (e.g., interannual variability), which may be instead affected by the low-frequency fluctuations of the radiative forcing, in radiation limited sites.

Acknowledgments

We would like to thank the Editor Desai and the two anonymous reviewers for their comments that significantly improved our manuscript. The authors are grateful to all individuals of the FLUXNET project (http://fluxnet.ornl.gov/) and the University of Michigan Biological Station (http://umbs.lsa.umich.edu/research/) involved in the collection of the data used in this study. A. Paschalis acknowledges the financial support of the Swiss National Sciences Foundation (grant P2EZP2_152244) and the Stavros Niarchos Foundation, through the SNSF Early Postdoc Mobility Fellowship. G. Katul acknowledges support from the National Science Foundation (NSF-AGS-1102227 and NSF-EAR-1344703), the United States Department of Agriculture (2011-67003-30222), and the U.S. Department of Energy through the Office of Biological and Environmental Research Terrestrial Carbon Processes program (DE-SC0006967 and DE-SC0011461). V. Ivanov was supported by the NSF grant EAR 1151443.

References

Allan, R. P., and B. J. Soden (2008), Atmospheric warming and the amplification of precipitation extremes, *Science*, *321*, 1481–1484, doi:10.1126/science.1160787.

Amenu, G. G., and P. Kumar (2008), A model for hydraulic redistribution incorporating coupled soil-root moisture transport, *Hydrol. Earth Syst. Sci.*, *12*(1), 55–74, doi:10.5194/hess-12-55-2008.

Araújo, A. C. et al. (2002), Comparative measurements of carbon dioxide fluxes from two nearby towers in a central Amazonian rainforest: The Manaus LBA site, *J. Geophys. Res.*, *107*(D20), 8090, doi:10.1029/2001JD000676.

Arora, V. K., et al. (2013), Carbon–concentration and carbon–climate feedbacks in CMIP5 Earth system models, *J. Clim.*, *26*(15), 5289–5314, doi:10.1175/JCLI-D-12-00494.1.

Asseng, S., I. Foster, and N. C. Turner (2011), The impact of temperature variability on wheat yields, *Global Chang. Biol.*, *17*(2), 997–1012, doi:10.1111/j.1365-2486.2010.02262.x.

Babst, F., et al. (2013), Site- and species-specific responses of forest growth to climate across the European continent, *Global Ecol. Biogeogr.*, *22*(6), 706–717, doi:10.1111/geb.12023.

Baldocchi, D., E. Falge, and K. Wilson (2000), A spectral analysis of biosphere-atmosphere trace gas flux densities and meteorological variables across hour to multi-year time scales, *Agric. For. Meteorol.*, *2915*, 1–27.

Baldocchi, D., et al. (2001), FLUXNET: A new tool to study the temporal and spatial variability of ecosystem-scale carbon dioxide, water vapor, and energy flux densities, *Bull. Am. Meteorol. Soc.*, *82*(4), 2415–2434.

Boer, G. J. (2009), Changes in interannual variability and decadal potential predictability under global warming, *J. Clim.*, *22*(11), 3098–3109, doi:10.1175/2008JCLI2835.1.

Bohrer, G., H. Mourad, T. A. Laursen, D. Drewry, R. Avissar, D. Poggi, R. Oren, and G. G. Katul (2005), Finite element tree crown hydrodynamics model (FETCH) using porous media flow within branching elements: A new representation of tree hydrodynamics, *Water Resour. Res.*, *41*, W11404, doi:10.1029/2005WR004181.

Bonan, G. B. (2008), Forests and climate change: Forcings, feedbacks, and the climate benefits of forests, *Science*, *320*(5882), 1444–1449, doi:10.1126/science.1155121.

Bonan, G. B., P. J. Lawrence, K. W. Oleson, S. Levis, M. Jung, M. Reichstein, D. M. Lawrence, and S. C. Swenson (2011), Improving canopy processes in the Community Land Model version 4 (CLM4) using global flux fields empirically inferred from FLUXNET data, *J. Geophys. Res.*, *116*, G02014, doi:10.1029/2010JG001593.

Bonan, G. B., K. W. Oleson, R. A. Fisher, G. Lasslop, and M. Reichstein (2012), Reconciling leaf physiological traits and canopy flux data: Use of the TRY and FLUXNET databases in the Community Land Model version 4, *J. Geophys. Res.*, *117*, G02026, doi:10.1029/2011JG001913.

Brooks, P. D., P. A. Troch, M. Durcik, E. Gallo, and M. Schlegel (2011), Quantifying regional scale ecosystem response to changes in precipitation: Not all rain is created equal, *Water Resour. Res.*, *47*, W00J08, doi:10.1029/2010WR009762.

Caldwell, M., and J. Richards (1986), Competing root systems: Morphology and models of absorption, in *On the Economy of Plant Form and Function*, pp. 251–273, Cambridge Univ. Press, Cambridge, U. K.

Cattiaux, J., H. Douville, R. Schoetter, S. Parey, and P. Yiou (2015), Projected increase in diurnal and interdiurnal variations of European summer temperatures, *Geophys. Res. Lett.*, *42*, 899–907, doi:10.1002/2014GL062531.

Collatz, G., J. Ball, C. Grivet, and J. Berry (1991), Physiological and environmental regulation of stomatal conductance, photosynthesis and transpiration: A model that includes a laminar boundary layer, *Agric. For. Meteorol.*, *54*(1074), 107–136.

Collatz, G., L. Bounoua, D. Randall, I. Fung, and P. Sellers (2000), A mechanism for the influence of vegetation on the response of the diurnal temperature range to changing climate Collatz in, *Geophys. Res. Lett.*, *27*(20), 3381–3384, doi:10.1029/1999GL010947.

Curtis, P., C. Vogel, C. Gough, H. Schmid, H. Su, and B. Bovard (2005), Respiratory carbon losses and the carbon-use efficiency of a northern hardwood forest, 1999–2003, *New Phytol.*, *617*(2), 437–456, doi:10.1111/j.1469-8137.2005.01438.x.

Dai, Y., R. Dickinson, and Y. Wang (2004), A two-big-leaf model for canopy temperature, photosynthesis, and stomatal conductance, *J. Clim.*, *17*, 2281–2299.

Daly, E., A. Porporato, and I. Rodríguez-Iturbe (2004), Coupled dynamics of photosynthesis, transpiration, and soil water balance. Part I: Upscaling from hourly to daily level, *J. Hydrometeorol.*, *5*(3), 546–558.

De Boeck, H. J., F. E. Dreesen, I. A. Janssens, and I. Nijs (2010), Climatic characteristics of heat waves and their simulation in plant experiments, *Global Change Biol.*, *16*(7), 1992–2000, doi:10.1111/j.1365-2486.2009.02049.x.

De Gonçalves, L. G. G., et al. (2013), Overview of the Large-Scale Biosphere–Atmosphere Experiment in Amazonia Data Model Intercomparison Project (LBA-DMIP), *Agric. For. Meteorol.*, *182–183*, 111–127, doi:10.1016/j.agrformet.2013.04.030.

Deardorff, J. W. (1978), Efficient prediction of ground surface temperature and moisture, with inclusion of a layer of vegetation, *J. Geophys. Res.*, *83*(C4), 1889–1903, doi:10.1029/JC083iC04p01889.

Dietze, M. C., et al. (2011), Characterizing the performance of ecosystem models across time scales: A spectral analysis of the North American Carbon Program site-level synthesis, *J. Geophys. Res.*, *116*, G04029, doi:10.1029/2011JG001661.

Donohue, R. J., M. L. Roderick, and T. R. McVicar (2007), On the importance of including vegetation dynamics in Budyko's hydrological model, *Hydrol. Earth Syst. Sci.*, *11*(2), 983–995, doi:10.5194/hess-11-983-2007.

Eagleson, P. (1978), Climate, soil, and vegetation: 1. Introduction to water balance dynamics, *Water Resour. Res.*, *14*(5), 705–712, doi:10.1029/WR014i005p00705.

Fang, J., S. Piao, Z. Tang, C. Peng, and W. Ji (2001), Interannual variability in net primary production and precipitation, *Science*, *293*, 1723, doi:10.1126/science.293.5536.1723a.

Farquhar, G., S. Caemmerer, and J. Berry (1980), A biochemical model of photosynthetic CO_2 assimilation in leaves of C 3 species, *Planta*, *90*, 78–90.

Fatichi, S. (2010), The modeling of hydrological cycle and its interaction with vegetation in the framework of climate change, Univ. of Florence, Univ. Braunschweig.

Fatichi, S., and S. Leuzinger (2013), Reconciling observations with modeling: The fate of water and carbon allocation in a mature deciduous forest exposed to elevated CO_2, *Agric. For. Meteorol.*, *174–175*, 144–157, doi:10.1016/j.agrformet.2013.02.005.

Fatichi, S., and V. Ivanov (2014), Interannual variability of evapotranspiration and vegetation productivity, *Water Resour. Res.*, *50*, 3275–3294, doi:10.1002/2013WR015044.

Fatichi, S., V. Y. Ivanov, and E. Caporali (2011), Simulation of future climate scenarios with a weather generator, *Adv. Water Resour.*, *34*(4), 448–467, doi:10.1016/j.advwatres.2010.12.013.

Fatichi, S., V. Y. Ivanov, and E. Caporali (2012a), A mechanistic ecohydrological model to investigate complex interactions in cold and warm water-controlled environments: 1. Theoretical framework and plot-scale analysis, *J. Adv. Model. Earth Syst.*, *4*, M05002, doi:10.1029/2011MS000086.

Fatichi, S., V. Y. Ivanov, and E. Caporali (2012b), A mechanistic ecohydrological model to investigate complex interactions in cold and warm water-controlled environments: 2. Spatiotemporal analyses, *J. Adv. Model. Earth Syst.*, *4*, M05003, doi:10.1029/2011MS000087.

Fatichi, S., M. J. Zeeman, J. Fuhrer, and P. Burlando (2014a), Ecohydrological effects of management on subalpine grasslands: From local to catchment scale, *Water Resour. Res.*, *50*, 148–164, doi:10.1002/2013WR014535.

Fatichi, S., S. Leuzinger, and C. Körner (2014b), Moving beyond photosynthesis: From carbon source to sink-driven vegetation modeling, *New Phytol.*, *201*(4), 1086–2095, doi:10.1111/nph.12614.

Fatichi, S., P. Molnar, T. Mastrotheodoros, and P. Burlando (2015), Diurnal and seasonal changes in near-surface humidity in a complex orography, *J. Geophys. Res. Atmos.*, *120*, 2358–2374, doi:10.1002/2014JD022537.

Fay, P. A., J. D. Carlisle, A. K. Knapp, J. M. Blair, and S. L. Collins (2000), Altering rainfall timing and quantity in a mesic grassland ecosystem: Design and performance of rainfall manipulation shelters, *Ecosystems*, *3*(3), 308–319, doi:10.1007/s100210000028.

Fay, P. A., J. M. Blair, M. D. Smith, J. B. Nippert, J. D. Carlisle, and A. K. Knapp (2011), Relative effects of precipitation variability and warming on tallgrass prairie ecosystem function, *Biogeosciences*, *8*(10), 3053–3068, doi:10.5194/bg-8-3053-2011.

Fisher, R., N. McDowell, D. Purves, P. Moorcroft, S. Sitch, P. Cox, C. Huntingford, P. Meir, and F. I. Woodward (2010), Assessing uncertainties in a second-generation dynamic vegetation model caused by ecological scale limitations, *New Phytol.*, *187*(3), 666–681, doi:10.1111/j.1469-8137.2010.03340.x.

Friedlingstein, P., M. Meinshausen, V. K. Arora, C. D. Jones, A. Anav, S. K. Liddicoat, and R. Knutti (2014), Uncertainties in CMIP5 climate projections due to carbon cycle feedbacks, *J. Clim.*, *27*(2), 511–526, doi:10.1175/JCLI-D-12-00579.1.

Gonzalez, P., R. P. Neilson, J. M. Lenihan, and R. J. Drapek (2010), Global patterns in the vulnerability of ecosystems to vegetation shifts due to climate change, *Global Ecol. Biogeogr.*, *19*(6), 755–768, doi:10.1111/j.1466-8238.2010.00558.x.

Gough, C. M., C. S. Vogel, H. P. Schmid, and P. S. Curtis (2008), Controls on annual forest carbon storage: Lessons from the past and predictions for the future, *BioScience*, *58*(7), 609–622, doi:10.1641/B580708.

Gough, C., B. Hardiman, L. Nave, G. Bohrer, K. D. Maurer, C. S. Vogel, K. J. Nadelhoffer, and P. S. Curtis (2013), Sustained carbon uptake and storage following moderate disturbance in a Great Lakes forest, *Ecol. Appl.*, *23*(5), 1202–1215, doi:10.1890/12-1554.1.

Gu, G., and R. F. Adler (2011), Precipitation and temperature variations on the interannual time scale: Assessing the impact of ENSO and volcanic eruptions, *J. Clim.*, *24*(9), 2258–2270, doi:10.1175/2010JCLI3727.1.

Haxeltine, A., and I. Prentice (1996), BIOME3: An equilibrium terrestrial biosphere model based on ecophysiological constraints, resource availability, and competition among plant functional types, *Global Biogeochem. Cycles*, *10*(4), 693–709, doi:10.1029/96GB02344.

He, L., V. Ivanov, G. Bohrer, J. E. Thomsen, C. S. Vogel, and M. Moghaddam (2013), Temporal dynamics of soil moisture in a northern temperate mixed successional forest after a prescribed intermediate disturbance, *Agric. For. Meteorol.*, *180*, 22–33, doi:10.1016/j.agrformet.2013.04.014.
Heisler-White, J. L., A. K. Knapp, and E. F. Kelly (2008), Increasing precipitation event size increases aboveground net primary productivity in a semi-arid grassland, *Oecologia*, *158*(1), 129–140, doi:10.1007/s00442-008-1116-9.
Hutyra, L. R., J. W. Munger, S. R. Saleska, E. Gottlieb, B. C. Daube, A. L. Dunn, D. F. Amaral, P. B. de Camargo, and S. C. Wofsy (2007), Seasonal controls on the exchange of carbon and water in an Amazonian rain forest, *J. Geophys. Res.*, *112*, G03008, doi:10.1029/2006JG000365.
Huxman, T. E., et al. (2004a), Convergence across biomes to a common rain-use efficiency, *Nature*, *429*, 651–654, doi:10.1038/nature02561.
Huxman, T. E., K. A. Snyder, D. Tissue, A. J. Leffler, K. Ogle, W. T. Pockman, D. R. Sandquist, D. L. Potts, and S. Schwinning (2004b), Precipitation pulses and carbon fluxes in semiarid and arid ecosystems, *Oecologia*, *141*(2), 254–268, doi:10.1007/s00442-004-1682-4.
Intergovernmental Panel on Climate Change (2013), *Climate Change 2013 The Physical Science Basis Working Group I Contribution to the Fifth Assessment Report of the Intergovernmental Panel on Climate Change*, Cambridge Univ. Press, Cambridge, U. K.
Ivanov, V. Y., R. L. Bras, and E. R. Vivoni (2008), Vegetation-hydrology dynamics in complex terrain of semiarid areas: 1. A mechanistic approach to modeling dynamic feedbacks, *Water Resour. Res.*, *44*, W03429, doi:10.1029/2006WR005588.
Ivanov, V. Y., S. Fatichi, G. D. Jenerette, J. F. Espeleta, P. A. Troch, and T. E. Huxman (2010), Hysteresis of soil moisture spatial heterogeneity and the "homogenizing" effect of vegetation, *Water Resour Res.*, *46*, W09521, doi:10.1029/2009WR008611.
Ivanov, V. Y., L. R. Hutyra, S. C. Wofsy, J. W. Munger, S. R. Saleska, R. C. de Oliveira, and P. B. de Camargo (2012), Root niche separation can explain avoidance of seasonal drought stress and vulnerability of overstory trees to extended drought in a mature Amazonian forest, *Water Resour. Res.*, *48*, W12507, doi:10.1029/2012WR011972.
Jentsch, A., J. Kreyling, and C. Beierkuhnlein (2007), A new generation of climate-change experiments: Events, not trends, *Front. Ecol. Envoron.*, *5*(7), 365–374, doi:10.1890/1540-9295(2007)5[365:ANGOCE]2.0.CO;2.
Joslin, J., M. Wolfe, and P. Hanson (2000), Effects of altered water regimes on forest root systems, *New Phytol.*, *147*(1), 117–129, doi:10.1046/j.1469-8137.2000.00692.x.
Karl, T., R. Knight, and N. Plummer (1995), Trends in high-frequency climate variability in the twentieth century, *Nature*, *377*, 217–220.
Kattge, J., and W. Knorr (2007), Temperature acclimation in a biochemical model of photosynthesis: A reanalysis of data from 36 species, *Plant. Cell Environ.*, *30*(9), 1176–1190, doi:10.1111/j.1365-3040.2007.01690.x.
Katul, G. G., C. T. Lai, K. Schäfer, B. Vidakovic, J. Albertson, D. Ellsworth, and R. Oren (2001), Multiscale analysis of vegetation surface fluxes: From seconds to years, *Adv. Water Resour.*, *24*(9–10), 1119–1132, doi:10.1016/S0309-1708(01)00029-X.
Katul, G. G., A. Porporato, E. Daly, A. C. Oishi, H.-S. Kim, P. C. Stoy, J.-Y. Juang, and M. B. Siqueira (2007a), On the spectrum of soil moisture from hourly to interannual scales, *Water Resour. Res.*, *43*, W05428, doi:10.1029/2006WR005356.
Katul, G. G., A. Porporato, and R. Oren (2007b), Stochastic dynamics of plant-water interactions, *Annu. Rev. Ecol. Evol. Syst.*, *38*(1), 767–791, doi:10.1146/annurev.ecolsys.38.091206.095748.
Kayler, Z. E., H. J. De Boeck, S. Fatichi, J. M. Grünzweig, L. Merbold, C. Beier, N. McDowell, and J. S. Dukes (2015), Experiments to confront the environmental extremes of climate change, *Front. Ecol. Environ.*, *13*(4), 219–225, doi:10.1890/140174.
Keefer, T. O., M. S. Moran, and G. B. Paige (2008), Long-term meteorological and soil hydrology database, Walnut Gulch Experimental Watershed, Arizona, United States, *Water Resour. Res.*, *44*, W05S07, doi:10.1029/2006WR005702.
Kharin, V. V., F. W. Zwiers, X. Zhang, and M. Wehner (2013), Changes in temperature and precipitation extremes in the CMIP5 ensemble, *Clim. Change*, *119*(2), 345–357, doi:10.1007/s10584-013-0705-8.
Kim, Y., R. G. Knox, M. Longo, D. Medvigy, L. R. Hutyra, E. H. Pyle, S. C. Wofsy, R. L. Bras, and P. R. Moorcroft (2012), Seasonal carbon dynamics and water fluxes in an Amazon rainforest, *Global Change Biol.*, *18*(4), 1322–1334, doi:10.1111/j.1365-2486.2011.02629.x.
Knapp, A. K., and M. D. Smith (2001), Variation among biomes in temporal dynamics of aboveground primary production, *Science*, *291*(5503), 481–484, doi:10.1126/science.291.5503.481.
Knapp, A. K., et al. (2008), Consequences of more extreme precipitation regimes for terrestrial ecosystems, *BioScience*, *58*(9), 811–821, doi:10.1641/B580908.
Kolari, P., J. Pumpanen, U. Rannik, H. Ilvesniemi, P. Hari, and F. Berninger (2004), Carbon balance of different aged Scots pine forests in Southern Finland, *Global Change Biol.*, *10*(7), 1106–1119, doi:10.1111/j.1365-2486.2004.00797.x.
Körner, C. (2009), Responses of humid tropical trees to rising CO_2, *Annu. Rev. Ecol. Evol. Syst.*, *40*(1), 61–79, doi:10.1146/annurev.ecolsys.110308.120217.
Körner, C. (2015), Paradigm shift in plant growth control, *Curr. Opin. Plant Biol.*, *25*, 107–114, doi:10.1016/j.pbi.2015.05.003.
Krinner, G., N. Viovy, N. de Noblet-Ducoudré, J. Ogée, J. Polcher, P. Friedlingstein, P. Ciais, S. Sitch, and I. C. Prentice (2005), A dynamic global vegetation model for studies of the coupled atmosphere-biosphere system, *Global Biogeochem. Cycles*, *19*, GB1015, doi:10.1029/2003GB002199.
Laio, F., A. Porporato, L. Ridol, and I. Rodriguez-iturbe (2001), Plants in water-controlled ecosystems: Active role in hydrologic processes and response to water stress II. Probabilistic soil moisture dynamics, *Adv. Water Resour.*, *24*(7), 707–723.
Li, D., M. Pan, Z. Cong, L. Zhang, and E. Wood (2013), Vegetation control on water and energy balance within the Budyko framework, *Water Resour. Res.*, *49*, 969–976, doi:10.1002/wrcr.20107.
Loik, M. E., D. D. Breshears, W. K. Lauenroth, and J. Belnap (2004), A multi-scale perspective of water pulses in dryland ecosystems: Climatology and ecohydrology of the western USA, *Oecologia*, *141*(2), 269–281, doi:10.1007/s00442-004-1570-y.
Manoli, G., S. Bonetti, J.-C. Domec, M. Putti, G. Katul, and M. Marani (2014), Tree root systems competing for soil moisture in a 3D soil-plant model, *Adv. Water Resour.*, *66*, 32–42, doi:10.1016/j.advwatres.2014.01.006.
Markewitz, D., S. Devine, E. A. Davidson, P. Brando, and D. C. Nepstad (2010), Soil moisture depletion under simulated drought in the Amazon: Impacts on deep root uptake, *New Phytol.*, *187*(3), 592–607, doi:10.1111/j.1469-8137.2010.03391.x.
McDowell, N., et al. (2013), Evaluating theories of drought induced vegetation mortality using a multimodel–experiment framework, *New Phytol.*, *200*(2), 304–321, doi:10.1111/nph.12465.
McManus, J. F. (1999), A 0.5-million-year record of millennial-scale climate variability in the North Atlantic, *Science*, *283*(5404), 971–975, doi:10.1126/science.283.5404.971.
Medvigy, D., and C. Beaulieu (2012), Trends in daily solar radiation and precipitation coefficients of variation since 1984, *J. Clim.*, *25*(4), 1330–1339, doi:10.1175/2011JCLI4115.1.
Medvigy, D., S. C. Wofsy, J. W. Munger, and P. R. Moorcroft (2010), Responses of terrestrial ecosystems and carbon budgets to current and future environmental variability, *Proc. Natl. Acad. Sci. U.S.A.*, *107*(18), 8275–8280, doi:10.1073/pnas.0912032107.
Mendel, M., S. Hergarten, and H. J. Neugebauer (2002), On a better understanding of hydraulic lift: A numerical study, *Water Resour. Res.*, *38*(10), 1183, doi:10.1029/2001WR000911.

Molini, A., G. G. Katul, and A. Porporato (2009), Revisiting rainfall clustering and intermittency across different climatic regimes, *Water Resour. Res.*, *45*, W11403, doi:10.1029/2008WR007352.
Moorcroft, P. R. (2006), How close are we to a predictive science of the biosphere?, *Trends Ecol. Evol.*, *21*(7), 400–407, doi:10.1016/j.tree.2006.04.009.
Myneni, R. B., et al. (2007), Large seasonal swings in leaf area of Amazon rainforests, *Proc. Natl. Acad. Sci. U.S.A.*, *104*(12), 4820–4823, doi:10.1073/pnas.0611338104.
Nagler, P. L., E. P. Glenn, H. Kim, W. Emmerich, R. L. Scott, T. E. Huxman, and A. R. Huete (2007), Relationship between evapotranspiration and precipitation pulses in a semiarid rangeland estimated by moisture flux towers and MODIS vegetation indices, *J. Arid Environ.*, *70*(3), 443–462, doi:10.1016/j.jaridenv.2006.12.026.
Nakai, T., G. Katul, A. Kotani, Y. Igarashi, T. Ohta, M. Suzuki, and T. Kumagai (2014), Radiative and precipitation controls on root zone soil moisture spectra, *Geophys. Reseach Lett.*, *41*, 7546–7554, doi:10.1002/2014GL061745.
Nepstad, D., C. de Carvalho, E. Davidson, P. Jipp, P. Lefebvre, G. Negreiros, E. da Silva, T. Stone, S. E. Trumbore, and S. Vieira (1994), The role of deep roots in the hydrological and carbon cycles of Amazonian forests and pastures, *Nature*, *372*, 666–669, doi:10.1038/372666a0.
Neumann, R., and Z. Cardon (2012), The magnitude of hydraulic redistribution by plant roots: A review and synthesis of empirical and modeling studies, *New Phytol.*, *194*, 337–352.
Norris, J. R., and M. Wild (2007), Trends in aerosol radiative effects over Europe inferred from observed cloud cover, solar "dimming," and solar "brightening", *J. Geophys. Res.*, *112*, D08214, doi:10.1029/2006JD007794.
Noy-Meir, I. (1973), Desert ecosystems: Environment and producers, *Annu. Rev. Ecol. Syst.*, *4*(1973), 25–51.
O'Gorman, P., and T. Schneider (2009), The physical basis for increases in precipitation extremes in simulations of 21st-century climate change, *Proc. Natl. Acad. Sci. U.S.A.*, *106*(35), 14,773–14,777, doi:10.1073/pnas.0907610106.
Oishi, A. C., R. Oren, K. A. Novick, S. Palmroth, and G. G. Katul (2010), Interannual invariability of forest evapotranspiration and its consequence to water flow downstream, *Ecosystems*, *13*(3), 421–436, doi:10.1007/s10021-010-9328-3.
Oleson, K. W. et al. (2013), Technical description of version 4.5 of the Community Land Model (CLM), Boulder, Colo.
Oliveira, R. S., T. E. Dawson, S. S. O. Burgess, and D. C. Nepstad (2005), Hydraulic redistribution in three Amazonian trees, *Oecologia*, *145*(3), 354–63, doi:10.1007/s00442-005-0108-2.
Oren, R., et al. (2001), Soil fertility limits carbon sequestration by forest ecosystems in a CO_2-enriched atmosphere, *Nature*, *411*, 469–472, doi:10.1038/35078064.
Palmroth, S., C. A. Maier, H. R. McCarthy, A. C. Oishi, H.-S. Kim, K. H. Johnsen, G. G. Katul, and R. Oren (2005), Contrasting responses to drought of forest floor CO_2 efflux in a Loblolly pine plantation and a nearby Oak-Hickory forest, *Global Change Biol.*, *11*(3), 421–434, doi:10.1111/j.1365-2486.2005.00915.x.
Palmroth, S., G. G. Katul, C. A. Maier, E. Ward, S. Manzoni, and G. Vico (2013), On the complementary relationship between marginal nitrogen and water-use efficiencies among Pinus taeda leaves grown under ambient and CO_2-enriched environments, *Ann. Bot.*, *111*(3), 467–477, doi:10.1093/aob/mcs268.
Papalexiou, S. M., D. Koutsoyiannis, and C. Makropoulos (2013), How extreme is extreme? An assessment of daily rainfall distribution tails, *Hydrol. Earth Syst. Sci.*, *17*, 851–862, doi:10.5194/hess-17-851-2013.
Pappas, C., S. Fatichi, S. Leuzinger, A. Wolf, and P. Burlando (2013), Sensitivity analysis of a process-based ecosystem model: Pinpointing parameterization and structural issues, *J. Geophys. Res. Biogeosciences*, *118*, 505–528, doi:10.1002/jgrg.20035.
Pappas, C., S. Fatichi, S. Rimkus, P. Burlando, and M. O. Huber (2015), The role of local scale heterogeneities in terrestrial ecosystem modeling, *J. Geophys. Res. Biogeosciences*, *120*, 341–360, doi:10.1002/2014JG002735.
Paschalis, A. (2013), Modelling the space time structure of precipitation and its impact on basin response, ETH Zurich, Diss no. 21112.
Paschalis, A., P. Molnar, S. Fatichi, and P. Burlando (2013), A stochastic model for high resolution space-time precipitation simulation, *Water Resour. Res.*, *49*, 8400–8417, doi:10.1002/2013WR014437.
Paschalis, A., P. Molnar, S. Fatichi, and P. Burlando (2014a), On temporal stochastic modeling of precipitation, nesting models across scales, *Adv. Water Resour.*, *63*, 152–166, doi:10.1016/j.advwatres.2013.11.006.
Paschalis, A., S. Fatichi, P. Molnar, S. Rimkus, and P. Burlando (2014b), On the effects of small scale space–time variability of rainfall on basin flood response, *J. Hydrol.*, *514*, 313–327, doi:10.1016/j.jhydrol.2014.04.014.
Peng, S., et al. (2013), Asymmetric effects of daytime and night-time warming on Northern Hemisphere vegetation, *Nature*, *501*(7465), 88–92, doi:10.1038/nature12434.
Peters, D. (2000), Climatic variation and simulated patterns in seedling establishment of two dominant grasses at a semi-arid arid-grassland ecotone, *J. Veg. Sci.*, *44*(4), 493–504, doi:10.2307/3246579.
Porporato, A., E. Daly, and I. Rodriguez-Iturbe (2004), Soil water balance and ecosystem response to climate change, *Am. Nat.*, *164*(5), 625–632, doi:10.1086/424970.
Pregitzer, K., R. Hendrick, and R. Fogel (1993), The demography of fine roots in response to patches of water and nitrogen, *New Phytol.*, *125*(3), 575–580.
Press, W., S. Teukolsky, W. Vetterling, and B. Flanner (1992), *Numerical Recepies*, Cambridge Univ. Press, Cambridge, U. K.
Pritchard, S. G., A. E. Strand, M. L. McCormack, M. A. Davis, A. C. Finzi, R. B. Jackson, R. Matamala, H. H. Rogers, and R. Oren (2008), Fine root dynamics in a loblolly pine forest are influenced by free-air-CO_2-enrichment: A six-year-minirhizotron study, *Global Change Biol.*, *14*(3), 588–602, doi:10.1111/j.1365-2486.2007.01523.x.
Pumpanen, J., H. Ilvesniemi, M. Perämäki, and P. Hari (2003), Seasonal patterns of soil CO_2 efflux and soil air CO_2 concentration in a Scots pine forest: Comparison of two chamber techniques, *Global Change Biol.*, *9*(3), 371–382.
Reichmann, L., O. Sala, and D. Peters (2013), Precipitation legacies in desert grassland primary production occur through previous-year tiller density, *Ecology*, *94*(2), 435–443, doi:10.1890/12-1237.1.
Reichstein, M., et al. (2013), Climate extremes and the carbon cycle, *Nature*, *500*(7462), 287–95, doi:10.1038/nature12350.
Renard, K. G., M. H. Nichols, D. A. Woolhiser, and H. B. Osborn (2008), A brief background on the U.S. Department of Agriculture Agricultural Research Service Walnut Gulch Experimental Watershed, *Water Resour. Res.*, *44*, W05S02, doi:10.1029/2006WR005691.
Restrepo-Coupe, N., et al. (2013), What drives the seasonality of photosynthesis across the Amazon basin? A cross-site analysis of eddy flux tower measurements from the Brasil flux network, *Agric. For. Meteorol.*, *182–183*, 128–144, doi:10.1016/j.agrformet.2013.04.031.
Ridolfi, L., P. D'Odorico, A. Porporato, and I. Rodriguez-Iturbe (2000), Impact of climate variability on the vegetation water stress, *J. Geophys. Res.*, *105*(D14), 13–18, doi:10.1029/2000JD900206.
Rigby, J. R., and A. Porporato (2008), Spring frost risk in a changing climate, *Geophys. Res. Lett.*, *35*, L12703, doi:10.1029/2008GL033955.
Ritchie, J. C., M. A. Nearing, M. H. Nichols, and C. A. Ritchie (2005), Patterns of soil erosion and redeposition on Lucky Hills watershed, Walnut Gulch Experimental Watershed, Arizona, *Catena*, *61*(2–3), 122–130, doi:10.1016/j.catena.2005.03.012.

Rodriguez-Iturbe, I., A. Porporato, F. Laio, and L. Ridol (2001), Plants in water-controlled ecosystems: Active role in hydrologic processes and response to water stress I. Scope and general outline, *Adv. Water Resour.*, *24*(7), 695–705.
Saleska, S. R., K. Didan, A. R. Huete, and H. R. da Rocha (2007), Amazon forests green-up during 2005 drought, *Science*, *318*(5850), 612, doi:10.1126/science.1146663.
Saleska, S., et al. (2003), Carbon in Amazon forests: Unexpected seasonal fluxes and disturbance-induced losses, *Science*, *302*(5650), 1554–1558.
Scott, R., W. Shuttleworth, T. O. Keefer, and A. Warrick (2000), Modeling multiyear observations of soil moisture recharge in the semiarid American Southwest, *Water Resour. Res.*, *36*(8), 2233–2247, doi:10.1029/2000WR900116.
Sellers, P., D. Randall, and G. Collatz (1996), A revised land surface parameterization (SiB2) for atmospheric GCMs. Part I: Model formulation, *J. Clim.*, *9*, 676–705.
Siqueira, M., G. G. Katul, and A. Porporato (2009), Soil moisture feedbacks on convection triggers: The role of soil–plant hydrodynamics, *J. Hydrometeorol.*, *10*(1), 96–112, doi:10.1175/2008JHM1027.1.
Sitch, S., et al. (2003), Evaluation of ecosystem dynamics, plant geography and terrestrial carbon cycling in the LPJ dynamic global vegetation model, *Global Change Biol.*, *9*(2), 161–185, doi:10.1046/j.1365-2486.2003.00569.x.
Sitch, S., et al. (2008), Evaluation of the terrestrial carbon cycle, future plant geography and climate-carbon cycle feedbacks using five Dynamic Global Vegetation Models (DGVMs), *Global Change Biol.*, *14*(9), 2015–2039, doi:10.1111/j.1365-2486.2008.01626.x.
Smith, N., et al. (2014), Toward a better integration of biological data from precipitation manipulation experiments into Earth system models, *Rev. Geophys.*, *52*, 412–434, doi:10.1002/2014RG000458.
Stoy, P. C., G. G. Katul, M. B. S. Siqueira, J.-Y. Juang, K. A. Novick, H. R. McCarthy, A. Christopher Oishi, J. M. Uebelherr, H.-S. Kim, and R. Oren (2006), Separating the effects of climate and vegetation on evapotranspiration along a successional chronosequence in the southeastern US, *Global Change Biol.*, *12*(11), 2115–2135, doi:10.1111/j.1365-2486.2006.01244.x.
Stoy, P. C., S. Palmroth, A. C. Oishi, M. B. S. Siqueira, J.-Y. Juang, K. A. Novick, E. J. Ward, G. G. Katul, and R. Oren (2007), Are ecosystem carbon inputs and outputs coupled at short time scales? A case study from adjacent pine and hardwood forests using impulse-response analysis, *Plant. Cell Environ.*, *30*(6), 700–710, doi:10.1111/j.1365-3040.2007.01655.x.
Stoy, P. C., et al. (2013), Evaluating the agreement between measurements and models of net ecosystem exchange at different times and timescales using wavelet coherence: An example using data from the North American Carbon Program Site-Level Interim Synthesis, *Biogeosciences*, *10*(11), 6893–6909, doi:10.5194/bg-10-6893-2013.
Sun, F., M. L. Roderick, and G. D. Farquhar (2012), Changes in the variability of global land precipitation, *Geophys. Res. Lett.*, *39*, L19402, doi:10.1029/2012GL053369.
Sun, Y., S. Solomon, A. Dai, and R. W. Portmann (2007), How often will it rain?, *J. Clim.*, *20*(19), 4801–4818, doi:10.1175/JCLI4263.1.
Suni, T., J. Rinne, A. Reissell, N. Altimir, P. Keronen, U. Rannik, M. Dal Maso, M. Kulmala, and T. Vesala (2003), Long-term measurements of surface fluxes above a Scots pine forest in Hyytiala, southern Finland, 1996–2001, *Boreal Environ. Res.*, *8*, 287–301.
Swemmer, A. M., A. K. Knapp, and H. A. Snyman (2007), Intra-seasonal precipitation patterns and above-ground productivity in three perennial grasslands, *J. Ecol.*, *95*(4), 780–788, doi:10.1111/j.1365-2745.2007.01237.x.
Thornton, P. K., P. J. Ericksen, M. Herrero, and A. J. Challinor (2014), Climate variability and vulnerability to climate change: A review, *Global Change Biol.*, *20*(11), 3313–3328, doi:10.1111/gcb.12581.
Tian, H., J. M. Melillo, D. W. Kicklighter, A. McGuire, J. Helfrich III, B. Moore III, and C. Vorosmarty (1998), Effect of interannual climate variability on carbon storage in Amazonian ecosystems, *Nature*, *396*, 664–667.
Todd-Brown, K. E. O., et al. (2014), Changes in soil organic carbon storage predicted by Earth system models during the 21st century, *Biogeosciences*, *11*(8), 2341–2356, doi:10.5194/bg-11-2341-2014.
Torrence, C., and G. Compo (1998), A practical guide to wavelet analysis, *Bull. Am. Meteorol. Soc.*, *79*(1), 61–78.
Vargas, R., M. S. Carbone, M. Reichstein, and D. D. Baldocchi (2010), Frontiers and challenges in soil respiration research: From measurements to model-data integration, *Biogeochemistry*, *102*(1–3), 1–13, doi:10.1007/s10533-010-9462-1.
Vico, G., et al. (2014), Climatic, ecophysiological, and phenological controls on plant ecohydrological strategies in seasonally dry ecosystems, *Ecohydrology*, *8*, 658–679, doi:10.1002/eco.1533, in press.
Vinnikov, K. Y. (2002), Diurnal and seasonal cycles of trends of surface air temperature, *J. Geophys. Res.*, *107*(D22), 4641, doi:10.1029/2001JD002007.
Volpe, V., M. Marani, J. D. Albertson, and G. Katul (2013), Root controls on water redistribution and carbon uptake in the soil-plant system under current and future climate, *Adv. Water Resour.*, *60*, 110–120, doi:10.1016/j.advwatres.2013.07.008.
Wan, S., Y. Luo, and L. L. Wallace (2002), Changes in microclimate induced by experimental warming and clipping in tallgrass prairie, *Global Change Biol.*, *8*(8), 754–768, doi:10.1046/j.1365-2486.2002.00510.x.
Wild, M., H. Gilgen, A. Roesch, A. Ohmura, C. N. Long, E. G. Dutton, B. Forgan, A. Kallis, V. Russak, and A. Tsvetkov (2005), From dimming to brightening: Decadal changes in solar radiation at Earth's surface, *Science*, *308*(5723), 847–850, doi:10.1126/science.1103215.
Williams, C. A., N. Hanan, R. J. Scholes, and W. Kutsch (2009), Complexity in water and carbon dioxide fluxes following rain pulses in an African savanna, *Oecologia*, *161*(3), 469–80, doi:10.1007/s00442-009-1405-y.
Wilson, K. B., and D. D. Baldocchi (2000), Seasonal and interannual variability of energy fluxes over a broadleaved temperate deciduous forest in North America, *Agric. For. Meteorol.*, *100*(1), 1–18, doi:10.1016/S0168-1923(99)00088-X.
Wilson, K., et al. (2002), Energy balance closure at FLUXNET sites, *Agric. For. Meteorol.*, *113*(1–4), 223–243, doi:10.1016/S0168-1923(02)00109-0.
Wohlfahrt, G., and L. Gu (2015), Opinion: The many meanings of gross photosynthesis and their implication for photosynthesis research from leaf to globe, *Plant. Cell Environ.*, doi:10.1111/pce.12569, in press.
Wu, Z., P. Dijkstra, G. W. Koch, J. Peñuelas, and B. A. Hungate (2011), Responses of terrestrial ecosystems to temperature and precipitation change: A meta-analysis of experimental manipulation, *Global Change Biol.*, *17*(2), 927–942, doi:10.1111/j.1365-2486.2010.02302.x.
Xia, J., J. Chen, S. Piao, P. Ciais, Y. Luo, and S. Wan (2014), Terrestrial carbon cycle affected by non-uniform climate warming, *Nat. Geosci.*, *7*(3), 173–180, doi:10.1038/ngeo2093.
Xu, C., N. G. McDowell, S. Sevanto, and R. A. Fisher (2013), Our limited ability to predict vegetation dynamics under water stress, *New Phytol.*, *200*(2), 298–300.
Yan, B., and R. Dickinson (2014), Modeling hydraulic redistribution and ecosystem response to droughts over the Amazon basin using Community Land Model 4.0 (CLM4), *J. Geophys. Res. Biogeosci.*, *119*, 2130–2143, doi:10.1002/2014JG002694.
Yuan, W., et al. (2007), Deriving a light use efficiency model from eddy covariance flux data for predicting daily gross primary production across biomes, *Agric. For. Meteorol.*, *143*(3–4), 189–207, doi:10.1016/j.agrformet.2006.12.001.
Yuan, Z. Y., and H. Chen (2010), Fine root biomass, production, turnover rates, and nutrient contents in boreal forest ecosystems in relation to species, climate, fertility, and stand age: Literature review and meta-analyses, *CRC Crit. Rev. Plant Sci.*, *29*(4), 204–221, doi:10.1080/07352689.2010.483579.